NASA CONTRACTOR REPORT

NASA CR-1065

NASA CR-1065

N68-26017

FACILITY FORM 602

(ACCESSION NUMBER) (THRU)

(PAGES) (CODE)

(NASA CR OR TMX OR AD NUMBER) (CATEGORY)

AN ANALYSIS OF THE COUPLED CHEMICALLY REACTING BOUNDARY LAYER AND CHARRING ABLATOR

JUN 1968
RECEIVED
NASA STI FACILITY
INPUT BRANCH

Part VI
An Approach for Characterizing Charring Ablator Response With In-Depth Coking Reactions

by Roald A. Rindal

Prepared by
ITEK CORPORATION, VIDYA DIVISION
Palo Alto, Calif.
for Manned Spacecraft Center

GPO PRICE $ _____

CFSTI PRICE(S) $ _____

Hard copy (HC) 3.00

Microfiche (MF) .65

ff 653 July 65

NATIONAL AERONAUTICS AND SPACE ADMINISTRATION • WASHINGTON, D. C. • JUNE 1968

NASA CR-1065

AN ANALYSIS OF THE COUPLED CHEMICALLY REACTING BOUNDARY LAYER AND CHARRING ABLATOR

Part VI

An Approach for Characterizing Charring Ablator Response With In-Depth Coking Reactions

By Roald A. Rindal

Distribution of this report is provided in the interest of information exchange. Responsibility for the contents resides in the author or organization that prepared it.

Issued by Originator as Aerotherm Report No. 66-7, Part VI

Prepared under Contract No. NAS 9-4599 by
ITEK CORPORATION, VIDYA DIVISION
Palo Alto, Calif.

for Manned Spacecraft Center

NATIONAL AERONAUTICS AND SPACE ADMINISTRATION

For sale by the Clearinghouse for Federal Scientific and Technical Information
Springfield, Virginia 22151 – CFSTI price $3.00

PRECEDING PAGE BLANK NOT FILMED.

FOREWORD

The present report is one of a series of six reports, published simultaneously, which describe analyses and computational procedures for: 1) prediction of the in-depth response of charring ablation materials, based on one-dimensional thermal streamtubes of arbitrary cross-section and considering general surface chemical and energy balances, and 2) nonsimilar solution of chemically reacting laminar boundary layers, with an approximate formulation for unequal diffusion and thermal diffusion coefficients for all species and with a general approach to the thermochemical solution of mixed equilibrium-nonequilibrium homogeneous or heterogeneous systems. Part I serves as a summary report and describes a procedure for coupling the charring ablator and boundary layer routines. The charring ablator procedure is described in Part II, whereas the fluid-mechanical aspects of the boundary layer and the boundary-layer solution procedure are treated in Part III. The approximation for multicomponent transport properties and the thermochemistry model are described in Parts IV and V, respectively. Finally, in Part VI an analysis is presented for the in-depth response of charring materials taking into account char-density buildup near the surface due to coking reactions in depth.

The titles in the series are:

Part I Summary Report: An Analysis of the Coupled Chemically Reacting Boundary Layer and Charring Ablator, by R. M. Kendall, E. P. Bartlett, R. A. Rindal, and C. B. Moyer.

Part II Finite Difference Solution for the In-depth Response of Charring Materials Considering Surface Chemical and Energy Balances, by C. B. Moyer and R. A. Rindal.

Part III Nonsimilar Solution of the Multicomponent Laminar Boundary Layer by an Integral Matrix Method, by E. P. Bartlett and R. M. Kendall.

Part IV A Unified Approximation for Mixture Transport properties for Multicomponent Boundary-Layer Applications, by E. P. Bartlett, R. M. Kendall, and R. A. Rindal.

Part V A General Approach to the Thermochemical Solution of Mixed Equilibrium-Nonequilibrium, Homogeneous or Heterogeneous Systems, by R. M. Kendall.

Part VI An Approach for Characterizing Charring Ablator Response with In-depth Coking Reactions, by R. A. Rindal.

This effort was conducted for the Structures and Mechanics Division of the Manned Spacecraft Center, National Aeronautics and Space Administration under Contract No. NAS9-4599 to Vidya Division of Itek Corporation with Mr. Donald M. Curry and Mr. George Strouhal as the NASA Technical Monitors. The work was initiated by the present authors while at Vidya and was completed by Aerotherm Corporation under subcontract to Vidya (P.O. 8471 V9002) after Aerotherm purchased the physical assets of the Vidya Thermodynamics Department. Dr. Robert M. Kendall of Aerotherm was the Program Manager and Principal Investigator.

PRECEDING PAGE BLANK NOT FILMED.

ABSTRACT

The analysis of a charring ablation material which may undergo subsurface coking of the pyrolysis gas is considered. Coking reactions considered include thermal cracking of gaseous hydrocarbons resulting in precipitation of carbon onto the char layer and, at higher temperatures, the subsequent internal chemical erosion of the char structure by the gaseous pyrolysis products. A generalized type of ablation material is defined which consists of inert, carbon, and reactive constituents. Three types of subsurface reactions are considered, 1) decomposition of up to three organic constituents to form initial char and pyrolysis gas products, 2) kinetically controlled decomposition of the pyrolysis gas resulting in carbon precipitation and char densification, and 3) at high temperatures, chemical erosion of the subsurface char matrix by the pyrolysis products according to the dictates of chemical equilibrium. A model is considered for evaluating the pressure distribution through the char layer of variable permeability. Differential equations are developed to represent the transfer of mass, energy, and momentum within the framework of the postulated phenomenological model, and the differential equations are subsequently cast into finite difference form suitable for coding into a computer program.

PRECEDING PAGE BLANK NOT FILMED.

TABLE OF CONTENTS

LIST OF FIGURES

LIST OF SYMBOLS

A	cross-sectional area
A_n	cross-sectional area through center of node n (Fig. 4)
a	generalized constituent (a = I,c,r)
B'_c	normalized char surface recession rate, $\dot{m}_c/\rho_e u_e C_M A$
B'_g	normalized pyrolysis gas mass flow rate at surface, $\dot{m}_g/\rho_e u_e C_M A$
C	carbon
E_i	activation energy for chemical kinetic equation for i^{th} reaction
I	inert constituent
K_i^o	mass fraction of constituent i relative to mass of constituent i in undecomposed material (i = 1,2,3)
K_a	mass fraction of constituent a relative to total mass (a = I,c,r)
$K^o_{c_{if}}$	mass of carbonaceous residue after complete decomposition per unit mass of constituent i prior to decomposition
$K^o_{c_i}$	mass fraction of elemental carbon in constituent i prior to decomposition
$\tilde{K}_{cg}$	total mass fraction of the element carbon (independent of molecular configuration) in the pyrolysis gas
K_p	equilibrium constant
$\tilde{K}_{cgE}$	total mass fraction of the element carbon in the pyrolysis gas (independent of molecular configuration) which would exist in equilibrium with condensed phase carbon
$\tilde{K}_k$	mass fraction of element k independent of molecular configuration
k_i	pre-exponential constant for kinetic decomposition equation
k_c	pre-exponential constant for kinetically controlled coking reactions
k	thermal conductivity
M_g	molecular weight of pyrolysis gas
m	mass
$m_{c_{io}}$	mass of elemental carbon in constituent i prior to decomposition
$m_{c_{if}}$	mass of elemental carbon in constituent i after complete decomposition

$\dot{m}_g$	pyrolysis gas flow rate
$\dot{m}_c$	char surface mass loss rate
n_i	reaction order for i^{th} reaction
n_c	reaction order for coking reaction
n	exponent in viscosity law (Eq. 80)
P	pressure
R	universal gas constant
r	generalized reactive constituent (r = i = 1,2,3)
S	distance from initial surface location to present surface location (Fig. 2)
$\dot{S}$	linear surface recession rate
T	temperature
T_o	reference temperature in viscosity relation (Eq. 80)
u_g	actual velocity of gas passing through the char
v	superficial gas velocity (Eq. 30)
x	coordinate fixed to receding surface (Fig. 2)
y	coordinate fixed to initial surface (Fig. 2)

GREEK

α	permeability coefficient (Eq. 29)
ϵ	interconnected void volume porosity
δ_n	thickness of node n
Δ	incremental change
β	gas momentum coefficient (Eq. 29)
ρ	density
$\rho_e u_e C_M$	boundary layer mass transfer coefficient
τ	time required for gas to pass through a node
μ	dynamic viscosity
μ_o	reference viscosity (Eq. 80)
θ	time

LIST OF SYMBOLS (Concluded)

SUBSCRIPTS

a	pertaining to constituent a
c	pertaining to carbon
coke	pertaining to coking reactions (forward or reverse)
Decom	pertaining to decomposition of organic solid
E	signifies chemical equilibrium
e	boundary layer edge conditions
f	pertaining to final (decomposed) state, also signifies forward rate coefficient
g	pyrolysis gas
i=1,2,3	particular reactive constituents
n	pertaining to node n (Fig. 4)
o	pertaining to initial (undecomposed) state
P	differentiation at constant pressure
p	pertaining to plastic
r	generalized reactive constituent
s	solid
T	differentiation at constant temperature
x	differentiation at constant x
y	differentiation at constant y

SUPERSCRIPT

o	pertaining to initial (undecomposed) state

AN APPROACH FOR CHARACTERIZING CHARRING ABLATOR RESPONSE WITH IN-DEPTH COKING REACTIONS

SECTION 1
INTRODUCTION

The theoretical characterization of ablation phenomena has received considerable attention during the past decade. Part II of the present series (Ref. 1) includes a partial bibliography on the subject which includes reference to a number of investigations directed toward mathematical characterization of various aspects relating to the subsurface behavior of particular material classes, to thermochemical interactions between a charring ablator and its environment, and to various material removal regimes which dictate the magnitude of surface recession. This report is directed toward a potentially important aspect of charring material response that has received little attention previously. Consideration is given to the ablation of a charring material which may undergo in-depth coking reactions and a mathematical formulation is proposed for systematically evaluating the extent and effects of forward and reverse coking reactions within the constraint of conserving chemical elements in-depth and at the heated surface. The equations are cast in finite difference form appropriate for coding into a computer program.

The mathematical model proposed herein represents an extension of that presented in References (1-4) in that certain chemical reactions between gaseous organic pyrolysis products and the char layer are considered. Experimental results presented in References 5 and 6 reveal that significant densification of the char layer may occur near the heated surface. The model described in this report is based upon the assumption that the densification results from a certain class of chemical reactions which cause a transfer of carbon between the pyrolysis products and the char layer. These reactions include the precipitation of carbon from the hydrocarbon containing pyrolysis products with attendant deposition upon the char (coking), and the reverse reaction evidenced by erosion of the carbonaceous char with attendant addition of carbon to the gaseous pyrolysis products. The forward and reverse coking reactions may occur in the low and high temperature regions of the char layer respectively, and are of interest because the permeability of the char layer is decreased by coking which may result in high gas pressures in depth. High pressure in depth may give rise to excessive char stress which may produce catastrophic failure of the char layer. The technique described herein includes consideration of internal pressure build-up resulting from pyrolysis product flow through a char layer, of variable permeability.

The model selected to represent the material state in depth is presented first, in Section 2; the conservation equations for chemical species, energy, and momentum are presented next, in Section 3; and are followed, in Section 4, by the finite difference representation of the differential equations.

SECTION 2
DESCRIPTION OF THE PHYSICAL PROCESS

In this section the type of ablative material being considered is described and the general types of reactions which are allowed to occur are identified. The model selected is believed to enable consideration of the most important thermochemical interactions controlling the in-depth response of a wide variety of ablation materials currently being considered for heat shielding applications.

In its undecomposed state the ablation material is taken to be composed of two basic types of constituents: 1) inert, and 2) reactive. The inert constituents will consist of materials which are not permitted to undergo molecular changes in depth, e.g., silica or other metal oxide reinforcements. The reactive constituents may consist of organic materials, carbon or graphite reinforcements, and water of crystalization of reinforcing fibers, for example. Carbon and graphite are included in the list of reactive constituents because they may be vaporized in depth or be eroded chemically by the gaseous products of other reactive constituent pyrolysis products. The following, idealized, irreversible reaction characterizes the initial decomposition of the composite.

$$\text{Inert} + \text{Reactive} \rightarrow \text{Inert} + \text{Carbon (S)} + \text{Gas (0)} \qquad (1)$$

As noted from this relation, the inert constituent does not take part in the reaction, but is simply transported from a constituent in the virgin plastic to a constituent in the initial decomposed material. The reactive constituents, on the other hand, do undergo a change in molecular configuration and phase, however, the products of this initial reaction may consist of only two constituents, solid carbon, and an initial pyrolysis gas (gas (0)). Reaction (1) should be looked upon as a reaction which splits the virgin material into three distinct parts, each having a fixed quantity of chemical elements. Previous investigations (e.g., Refs. 1-4) consider no further chemical reactions between the pyrolysis products and the char. Indeed, further decomposition of the pyrolysis gas to yield a different gas composition may be treated by previous models, but decomposition to yield precipitation of carbon onto the char (coking) may not be treated with these models. In the present formulation, the initial pyrolysis is treated by Reaction (1). The gas elemental composition resulting from this initial decomposition is fixed

but further reactions are allowed and will be discussed subsequently. It should be pointed out that even though the initial gas composition is fixed with respect to its elemental composition, its molecular composition will depend upon the temperature and pressure at the point where decomposition occurs. Ideally, the elemental composition of the gas evolved at a point should depend upon the particular reactive constituent which is undergoing decomposition at that point, e.g. for nylon-phenolic; nylon would decompose first to yield something like $C_6H_{11}ON$, which would be followed by decomposition of phenolic to yield something like C_3H_6O at higher temperature. The inclusion of such detailed considerations in a computational scheme, however, would represent a rather extensive effort which is not believed warranted for the small gain in accuracy which would result. The approach taken, therefore, is to consider the elemental composition of the initial pyrolysis gases to represent the elemental composition of all gaseous pyrolysis products taken collectively. The initial off-gas elemental composition, $\tilde{K}_{k,g,o}$, may then be obtained by subtracting the quantity of chemical elements contained in a laboratory produced char from the chemical elements contained in the virgin plastic.

$$\tilde{K}_{k,g,o} = \frac{m_p \tilde{K}_{kp} - m_c \tilde{K}_{kc}}{m_p - m_c} \qquad (2)$$

(k = H,C,N,O, e.g.)

where

$\tilde{K}_{k,g,o}$ represents the mass of element k per unit mass of gas initially evolved

m_p mass of virgin plastic sample

m_c mass of char after decomposing in an inert atmosphere at a moderate temperature (2,000 - 3,000°R)

$\tilde{K}_{kp}$ mass of element k per unit mass of virgin plastic

$\tilde{K}_{kc}$ mass of element k per unit mass of char.

After the initial decomposition gas is formed, it will percolate through the char layer toward the heated surface which will result in an increased gas temperature and decreased pressure. The change in pressure and temperature will cause the initial gas products (gas (0)) to undergo numerous chemical reactions as they pass through the char. The reactions considered here fall

into three general categories:

1. Decomposition of the gas including thermal decomposition of high-molecular-weight hydrocarbons and dissociation of CO_2, H_2O, and H_2 for example.
2. Further decomposition of the hydrocarbons resulting in precipitation of carbon (coking) on the adjacent char passages resulting in char density buildup.
3. Chemical erosion of the char layer (below the heated surface) by the gases including carbon vaporization resulting in a char density reduction near the heated surface.

The three reaction regimes are represented on the following sketch for decomposition of a hypothetical material.

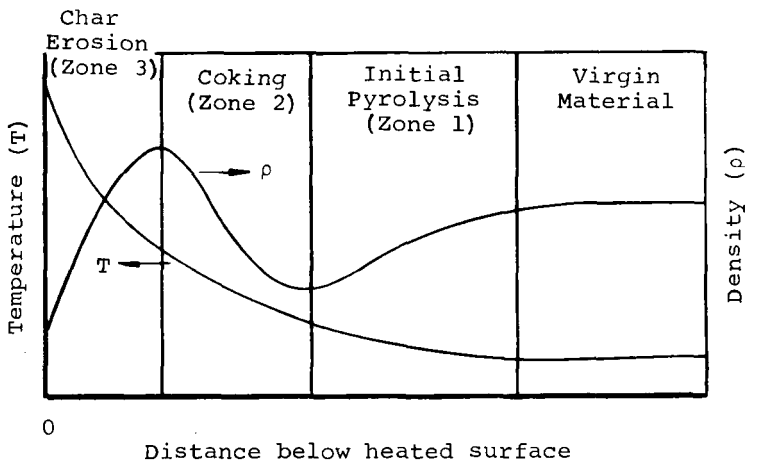

The classification of reactions above corresponds to the order in which the various types of reactions would be expected to occur as the gas passes through the char. The first class of reactions may be looked upon simply as the gas reacting with itself so no change in the concentration of chemical elements in the gas results, $\tilde{K}_{kg} = \tilde{K}_{kgo}$. The second two classes of reactions, however, will result in a transfer of carbon elements between the gas and the porous char. With regard to the elemental composition change these reactions may be considered reversible.

$$\text{gas (0)} \underset{3}{\overset{2}{\rightleftharpoons}} \text{gas + carbon (S)} \qquad (3)$$

where the forward reaction corresponds to moderate temperature, type 2 reactions, and results in a precipitation of carbon from the initial pyrolysis gas. The subsequent, type 3, high temperature reactions, result in char erosion with attendant addition of carbon to the gas.

An understanding of the detailed kinetic mechanisms required to characterize these reactions is not presently in hand; however, some qualitative information is available upon which a crude model may be formulated. The specific information relating to each reaction type is presented briefly and the physical model adapted to characterize each reaction regime is described in the following paragraphs.

Type 1 Reactions - If the subsurface composition is computed on the basis of chemical equilibrium considerations a far more dense char is predicted to occur than is observed from char density measurements (Ref. 2). It may be concluded either that condensed phase carbon is formed but does not stick to the char, or that the high molecular weight hydrocarbons do not decompose according to the dictates of chemical equilibrium. The latter possibility seems more probable but conclusive experimental evidence on this matter is lacking. It would seem appropriate to compute the initial gas phase elemental composition from Equation 2, and to evaluate the gas phase molecular composition by assuming gas phase chemical equilibrium and not consider condensed phase carbon as a possible product. Additional constraints must be placed upon the equilibrium calculation in order to eliminate other unlikely species from occurring as well. For example, mass spectrometer measurements presented in Reference 7 do not indicate the presence of any $C_{10}H$, C_9H_2, or C_8H, whereas these species are predicted to occur to a significant extent from equilibrium calculations for the resin system which was analyzed. By employing experimental techniques such as those reported in Reference 7, one should be able to identify those molecular species which will occur. The distribution of these experimentally verified species may then be obtained from equilibrium considerations.

Type 2 Reactions - A certain amount of experimental evidence exists (Refs. 5 and 6) which indicates that char densification may occur between the organic decomposition zone and the heated surface. It appears that this char densification is a result of deposition of condensed phase carbon from the hydrocarbons in the organic pyrolysis gas products. This seems reasonable since, as indicated above, the gases contain far more carbon than would exist if equilibrium were achieved. As the gases approach the heated surface their temperature is increased and the rate at which equilibrium is approached increases. In the present study, the rate at which equilibrium is approached is represented by a kinetic equation of the Arrhenius form. The rate at which

coking reactions may proceed is taken to be proportional to a forward rate coefficient and a driving potential represented by the difference in chemical composition between the actual gas composition and the equilibrium gas composition. Consider the reaction rate of coking methane gas, for example[1]

$$\dot{m}_{coke_{CH_4}} \propto k_f \left(P_{CH_4} - \frac{P_{H_2}^2}{K_p} \right) \tag{4}$$

where K_p is the equilibrium constant for the coking reaction

$$CH_4 \rightleftarrows 2H_2 + C\ (S) \tag{5}$$

Expressing the forward rate coefficient in Arrhenius form yields:

$$k_{f_i} = A_i\, e^{-E_i/R\,T} \tag{6}$$

where the frequency factor (A_i) and activation energy (E_i) are characteristic of the i^{th} reaction such as Reaction 5. The total coking rate from the gaseous pyrolysis products would be given by the sum of the coking rates attributable to each reaction.

$$\dot{m}_{coke} = \sum_i \dot{m}_{coke_i} \tag{7}$$

where i includes coking reactions for all hydrocarbon species present. The above technique for evaluating the coking rate, aside from requiring time-consuming computation procedures, would require specification of the physical constants, A_i and E_i, for each of the many reactions being considered. The rate would also depend critically upon the specific concentrations of each molecular species, and, as indicated earlier, the methods for their evaluation are not presently in hand. Alternatively, an approximate procedure is proposed here which has the following features:

1) It is simple enough to be included practically in a charring ablation solution.

---

[1] The reaction is presumed ideal so the partial pressure exponents are equal to the stoichiometric coefficients.

2) It approaches the coking rates which would be predicted by the more complete equations above when kinetics are relatively slow or fast.

3) It is based upon parameters which may be controlled in a laboratory experiment to derive data on the coking process.

The present procedure consists of specifying the coking rate as the product of a single forward rate coefficient and a carbon mass fraction "coking potential" which represents the net effect of all coking reactions such as Equation (6).

$$\dot{m}_{coke} \propto k_f(\tilde{K}_{cg} - \tilde{K}_{cgE}) \tag{8}$$

where the forward rate coefficient is expressed in Arrhenius form as above, and the driving potential is represented by the difference between the elemental carbon mass fraction of the gas and that which would exist if equilibrium were achieved.

Figure 1 depicts the elemental carbon content of a typical pyrolysis gas for the following situations: 1) for the initial pyrolysis gas (Equation (2), 2) for the pyrolysis gas if equilibrium were achieved, and 3) for a typical case utilizing the above model, all as functions of temperature. It is noted that at low temperatures (regime 1) the elemental carbon mass fraction remains unchanged until regime 2 is reached, at which point kinetically controlled coking reactions will cause the elemental carbon content to decrease until the equilibrium composition is reached. This marks the onset of regime 3 which is characterized by addition of carbon to the gas from the char.

Type 3 Reactions - In the event local char layer temperatures much in excess of 4500°R are achieved, it is probable that chemical equilibrium will be achieved between the pyrolysis gas and the char, in which case the coking potential will reach zero. For this reason type 3 reactions are presumed to occur in chemical equilibrium and sufficient carbon will be added to the gas from the char to maintain this equilibrium. This char erosion will result in a char density decrease which may, in an extreme case, cause the char density to approach zero.

SECTION 3
FORMULATION OF THE SUBSURFACE CONSERVATION EQUATIONS

The differential equations which characterize the conservation of species, momentum, and energy within a charring ablation material are presented in this section. The equations are based upon the physical model described above.

3.1 SPECIES CONSERVATION

In order to properly characterize the rates of plastic decomposition and pyrolysis gas coking in depth it is necessary to accurately assess the state of both the ablation material and the pyrolysis gases. The state of the ablation material depends upon the relative quantities of each constituent (reactive, inert, and carbon) and temperature whereas the state of the pyrolysis gas depends upon the gas carbon content, temperature, and pressure. Temperatures are obtained from the energy equation and pressures from the momentum equation, both of which are presented subsequently. The species conservation equations, presented here, relate the rate of change of ablation material composition and pyrolysis gas composition to decomposition and coking events throughout the decomposition zone and char layer.

As indicated earlier (Reactions 1 and 3) the ablation material may, at any point in space and time, be represented by a mixture of inert, reactive, and carbon species. The geometrical configuration considered is shown in Figure 2. Considering a control volume of extent Ady, the total mass may be expressed as

$$m = m_I + m_r + m_c + m_g \tag{9}$$

where

m_I = mass inert constituents

m_c = mass of condensed carbon

m_g = mass of gas

$m_r = \sum_{i=1,2,3} m_i$, mass of all i reactive constituents

It is noted that the mass of gas, m_g in the control volume is, in general, much smaller than the other masses so the total mass in the control volume may be written

$$m = \sum_a m_a \tag{10}$$

where $a = I, c, r$

and $r = 1, 2, 3$

It will be convenient later to consider a coordinate system fixed to the receding surface (x = const). With this in mind, the mass conservation equation is written for the moving coordinate system by differentiating equation (10) at constant x .

$$\left.\frac{\partial m}{\partial \theta}\right|_x = \frac{\partial}{\partial \theta}\left(\left.\sum_a m_a\right|_x\right) \tag{11}$$

The mass change rate of a constituent, a , may result from chemical reactions (organic decomposition, coking, or char erosion) and convection resulting from coordinate system movement. The mass change rate at constant x may be expressed in terms of the change resulting from chemical reactions and the change resulting from coordinate system motion. Functionally, the mass of constituent a may be written in terms of time and position.

$$m_a = m_a(\theta, y)$$

Applying the chain rule yields

$$dm_a = \left.\frac{\partial m_a}{\partial \theta}\right|_y d\theta + \left.\frac{\partial m_a}{\partial y}\right|_\theta dy$$

Differentiating with respect to time at constant x obtains

$$\left.\frac{\partial m_a}{\partial \theta}\right|_x = \left.\frac{\partial m_a}{\partial \theta}\right|_y + \left.\frac{\partial m_a}{\partial y}\right|_\theta \left.\frac{\partial y}{\partial \theta}\right|_x \tag{12}$$

The second term may be related to the surface recession rate by considering the coordinate system dependence of x on y .

$$y = x + S \tag{13}$$

From which,

$$\left.\frac{\partial y}{\partial \theta}\right|_x = \left.\frac{\partial S}{\partial \theta}\right|_x$$

but the surface recession, S , may be considered as a function of time alone, so:

$$\left.\frac{\partial S}{\partial \theta}\right|_x = \frac{dS}{d\theta} \equiv \dot{S} \tag{14}$$

Substitution of Equation (14) into Equation (12) and noting that differentiation with respect to x or y at constant time is equivalent, yields a conservation equation for condensed phase species below the surface.

$$\left.\frac{\partial m_a}{\partial \theta}\right|_x = \left.\frac{\partial m_a}{\partial \theta}\right|_y + \left.\frac{\partial m_a}{\partial x}\right|_\theta \dot{S} \tag{15}$$

The conservation equation for gaseous species in depth follows directly from consideration of the gas generation rate resulting from decomposition and the gas-to-condensed-phase transfer associated with coking reactions.

$$\left.\frac{\partial \dot{m}_{ga}}{\partial y}\right|_\theta = \frac{\partial}{\partial \theta}\,(\rho_a A)_y \tag{16}$$

As indicated in Section 1 (Reaction 1) the reactive constituents are presumed to decompose into a gas having a fixed elemental composition, given by Equation (2), and that subsequent gas phase reactions (coking or erosion) will have the sole effect of removing or adding elemental carbon to the gas. It is therefore necessary to keep track of only one element in the gas phase, elemental carbon. The gas phase conservation equation for elemental carbon, $a = c$, is

$$\frac{\partial}{\partial y}(\tilde{K}_{cg}\dot{m}_g)_\theta = \frac{\partial}{\partial \theta}(\tilde{K}_c \rho A)_y \tag{17}$$

The overall mass conservation equations for condensed and gas phase species follow directly from summing Equations (15) and (16) over all "a" species.

$$\left.\frac{\partial m}{\partial \theta}\right|_x = \left.\frac{\partial m}{\partial \theta}\right|_y + \left.\frac{\partial m}{\partial x}\right|_\theta \dot{S} \tag{18}$$

and

$$\left.\frac{\partial \dot{m}_g}{\partial y}\right|_\theta = \frac{\partial}{\partial \theta}\,(\rho A)_y \tag{19}$$

Evaluation of the convection term, $\left.\frac{\partial m_a}{\partial x}\right|_\theta \dot{S}$, in the species conservation equation is relatively straightforward; however, the term representing species change rates associated with chemical reactions, $\left.\frac{\partial m_a}{\partial \theta}\right|_y$, requires rather extensive consideration. For the inert species, $a = I$, the mass change rate resulting from chemical reactions is zero.

$$\left.\frac{\partial m_I}{\partial \theta}\right|_y = 0 \tag{20}$$

The treatment given the other constituents, a = r and c , is described in the following two subsections.

3.1.1 Species Conservation for Reactive Constituents (a = r)

The reactive constituents, r , are defined here as those constituents which may decompose to form gaseous and/or carbonaceous pyrolysis products

$$\text{Reactive} \rightarrow \text{Carbon (S)} + \text{Gas (O)} \tag{21}$$

The above, irreversible reaction is taken to proceed at a rate governed by an equation of the Arrhenius form for each of up to three reactive constituents

$$\left.\frac{\partial m_r}{\partial \theta}\right)_y = \sum_{i=1,2,3} m_{io} \left.\frac{\partial K_i^o}{\partial \theta}\right)_y \tag{22}$$

where

$$\left.\frac{\partial K_i^o}{\partial \theta}\right)_y = -k_i \, e^{-E_i/R\,T} \, (K_i^o)^{n_i} \tag{23}$$

and $K_i^o = \dfrac{m_i}{m_{i_o}}$, mass of constituent i per unit mass of constituent i prior to decomposition.

The form selected to represent the decomposition rate arises from a desire to express the kinetic coefficients in terms of quantities readily measureable in the laboratory. Equation (23) is developed in Appendix A in terms of quantities readily derived from TGA (thermogravimetric analysis) data.

Equations (22) and (23) enable evaluation of the term $\left.\frac{\partial m_a}{\partial \theta}\right)_y$ in the species conservation Equation (15) for decomposable reactive constituents (a = r). In order to evaluate this term for carbon (a = c) it is necessary to first consider all reactions which may involve carbon. This includes both the decomposition reactions just described, and coking reactions (forward and reverse). Coking reactions are discussed next.

3.1.2 Species Conservation for Carbon (a = c)

Carbon is generated in the charring material matrix when the virgin material decomposes as described above, and when coking reactions cause a transfer of carbon from the pyrolysis gas to the char (zone 2 described in Section 2 above). Carbon is removed from the charring material when reverse

coking reactions effect a transfer of carbon from the char to the pyrolysis gas (zone 3). The conservation of carbon species associated with decomposition is considered first, in Section 3.1.2.1, and is followed, in Section 3.1.2.2, by carbon conservation relations associated with forward and reverse coking reactions.

3.1.2.1 Organic Decomposition

From Equations (A-3) and (A-6) developed in Appendix A, it may be shown that the rate of production of carbonaceous residue from the i^{th} decomposition reaction is related to the rate of decomposition of constituent i, in the following manner

$$\left.\frac{\partial m_{ci}}{\partial \theta}\right)_y = - K^o_{c_{if}} \left.\frac{\partial m_i}{\partial \theta}\right)_y \tag{24}$$

where $K^o_{c_{if}} \equiv \frac{m_{c_{if}}}{m_{io}}$ is the mass of carbonaceous residue resulting from complete decomposition of constituent i, per unit mass of constituent i prior to decomposition. Summation of Equation (24) over all i yields the carbon production rate as a result of organic decomposition reactions.

$$\left.\frac{\partial m_c}{\partial \theta}\right)_{y,d} = \sum_{i=1,2,3} - K^o_{c_{if}} \, m_{io} \left.\frac{\partial K^o_i}{\partial \theta}\right)_y \tag{25}$$

where the subscript d signifies carbon production associated with organic decomposition (Reaction 21). Carbon addition to and removal from the char (coking reactions) are considered next.

3.1.2.2 Coking Reactions

Coking reactions, as employed here, refer to all chemical reactions which result in a transfer of carbon atoms between the pyrolysis gases and the char structure. This includes both type 2 and type 3 reactions introduced earlier in Section 2. Type 2 reactions include the normal class of coking reactions characterized by the deposition of carbon upon the char resulting from hydrocarbon decomposition. Type 3 reactions occur at much higher temperature where equilibrium dictates a reverse reaction characterized by erosion of the char resulting from vaporization and chemical attack by the pyrolysis gases.

3.1.2.2.1 Forward coking reactions

The physical model to be employed for characterizing the rate at which carbon is coked from the gas was introduced above, in Section 2. It is assumed that the pyrolysis gas composition changes at a rate dictated by an equation of the Arrhenius form.

$$\left.\frac{\partial \tilde{K}_{cg}}{\partial \theta}\right|_{y,K_i} = -k_c\, e^{-E_c/R\,T}\,(P)^{n_c}\,(\tilde{K}_{cg} - \tilde{K}_{cgE})^{n_c} \qquad (26)$$

where

$\tilde{K}_{cg}$ - mass fraction of carbon in the pyrolysis gas independent of molecular configuration

P - pressure

k_c, E_c, n_c - kinetic coefficients for coking reactions

$\tilde{K}_{cgE}$ - mass fraction of carbon in the pyrolysis gas which would exist if equilibrium were achieved at the local temperature and pressure

Equation (26) expresses the rate of change of carbon content in the gas in terms of a driving potential which approaches zero as equilibrium is achieved. The driving potential is noted to depend in a direct manner upon the system pressure as is believed appropriate for gas phase reactions. Partial differentiation of the gas carbon content is performed at constant y and constant K_i (composition of the plastic-char matrix where coking is occurring). It is expressed in this manner because coking is allowed to occur in regions of the char still undergoing decomposition. Since local pyrolysis results in the addition of fresh gas (having a carbon content, $\tilde{K}_{cgo}$) to the pyrolysis gas stream, it too affects the gas composition change rate. Equation (26) reflects the gas composition change rate resulting from coking alone. The total carbon change rate of the pyrolysis gas resulting from both decomposition and coking is given by adding the effects of that due to decomposition (Equation (22) and coking (Equation (26)). This addition is given consideration subsequently, in the finite difference formulation (Section 4).

3.1.2.2.2 Reverse coking reactions

Referring to Equation (26), it is noted that the coking rate approaches zero as gas phase equilibrium is achieved, i.e., as $(\tilde{K}_{cg} - \tilde{K}_{cgE}) \rightarrow 0$. When the coking potential reaches zero, $(\tilde{K}_{cg} - \tilde{K}_{cgE}) = 0$, the gas is assumed to

be in equilibrium with the char layer:

$$\widetilde{K}_{cg} = \widetilde{K}_{cgE} \tag{27}$$

where the pyrolysis gas equilibrium carbon content may be expressed as a function of temperature and pressure alone. The rate of change of elemental carbon content in the pyrolysis gas is then related to the temperature and pressure gradient.

$$\left.\frac{\partial \widetilde{K}_{cg}}{\partial y}\right|_{\theta} = \left.\frac{\partial \widetilde{K}_{cgE}}{\partial T}\right|_{P} \left.\frac{\partial T}{\partial y}\right|_{\theta} + \left.\frac{\partial \widetilde{K}_{cgE}}{\partial P}\right|_{T} \left.\frac{\partial P}{\partial y}\right|_{\theta} \tag{28}$$

The rate of char erosion by the pyrolysis gas (reverse coking) may then be obtained from Equations (28) and (17). This matter is given further consideration subsequently, in Section 4.

3.2 MOMENTUM EQUATION

The momentum equation is considered in depth in order to relate the gas flow rate in the char layer to the pressure distribution throughout the char layer. It is desired to evaluate the pressure at all points in the char layer for two reasons: 1) the coking reactions, both forward and reverse, are pressure dependent, and 2) evaluation of the pressure distribution through the char layer will enable determination of char stresses in an approximate manner.

In order to obtain an expression relating local pressure in the char layer to other pertinent variables it is useful to examine experimental data taken for a range of variation of the pertinent parameters of interest, and to deduce the most significant effects by generalizing this data.

The data presented by Green (Ref. 8) is employed for this purpose. Green presents a compilation of data for flow of various gases through a wide variety of porous media for a large range of flow conditions. In order to relate pressure gradients to viscous and inertial forces he employs the correlation equation first proposed by Reynolds.

$$\frac{dP}{dy} = \alpha \mu v + \beta \rho v^2 \tag{29}$$

where the first term represents viscous forces and the second, momentum forces. The quantities α and β are empirical coefficients, μ is the gas viscosity, and ρ is the gas density. The velocity in Equation (29) is a "superficial

velocity" defined on the basis of the gas flow rate per unit projected area in a plane normal to the velocity vector.

$$v \equiv \frac{\dot{m}_g}{\rho_g A} \tag{30}$$

Referring to Equation (29) the ratio of inertial to viscous forces may be written as:

$$\frac{\text{Inertial Force}}{\text{Viscous Force}} = \frac{\beta \dot{m}_g}{\alpha \mu A} \tag{31}$$

where $\dot{m}_g = \rho v$ is the gas flow rate per unit total area. The compilation of data presented by Green includes tabulations of the empirical coefficients α and β for a wide variety of porous media including packed beds of irregular and spherical particles ranging in nominal size from 0.08 inch to 0.1875 inch and for close packed wire screens ranging from 60 to 5 mesh. The nominal range of porosities included varies from 0.3 to 0.8. The experimentally derived coefficients α and β are shown in Figure 3 along with a straight line fit to the data.

$$\alpha = 0.794 \times 10^{4} \beta$$

where α has units of ft^{-2} and β has units of ft^{-1}. The correlation is not excellent, but appears appropriate for order-of-magnitude considerations. Substituting this relation into Equation (31) obtains

$$\frac{\text{Inertial Force}}{\text{Viscous Force}} = 1.26 \times 10^{-4} \frac{\dot{m}_g}{\mu A}$$

For the temperature range of interest ($2000^{\circ}R$ - $5000^{\circ}R$) the gas viscosity will range from about 0.3×10^{-4} to 0.5×10^{-4} lb/ft-sec. Considering a gas viscosity of 0.4×10^{-4} lb/ft-sec, the ratio of inertial to viscous forces may be written:

$$\frac{\text{Inertial Force}}{\text{Viscous Force}} = 3.15 \frac{\dot{m}_g}{A}$$

where $\dot{m}_g/A$ has the units of lb/ft^2-sec. It may therefore be concluded that for pyrolysis gas flow rates of 0.01 lb/ft^2-sec and less, the inertial terms may be ignored in which case Equation (29) reduces to Darcy's Law.

$$\frac{dP}{dy} = \alpha\mu v$$

where α^{-1} is the permeability. It is recommended, however, that the more complete correlation equation (29) be employed for pressure drop calculations in the char layer of ablating materials since it is valid for a wider range of conditions of practical interest.

3.3 ENERGY EQUATION

The subsurface energy equation for a charring ablator may be written in terms of a stationary coordinate system (see Fig. 2).

$$\overbrace{\frac{\partial}{\partial\theta}(\rho hA)_y}^{\text{storage}} = \frac{\partial}{\partial y}\left(kA\frac{\partial T}{\partial y}\right)_\theta + \frac{\partial}{\partial y}(\dot{m}_g h_g)_\theta \qquad \text{conduction} \qquad \text{convection} \qquad (32)$$

In Equation (32) the rate of energy storage term is expressed in terms of the material density, ρ , and specific enthalpy, h , at a point. The implicit assumption in such a formulation is that the density and enthalpy are sufficient properties to represent the material state. This is indeed possible when considering simple irreversible decomposition of the plastic into char and gas (see e.g. Refs. 1-4), but when further reactions accompanied by mass transfer between the char and gas are considered, the density and enthalpy alone are not sufficient properties to establish the material state. It is therefore desired for the present analysis to express Equation (32) in terms of quantities sufficient to define the state for the situation where mass transfer may occur between the pyrolysis gas and the char. It is also most expedient if these quantities are readily accessible in the computation scheme. These considerations have led to the selection of the mass of constituent a , in a control volume (m_a) and specific enthalpy of component a (h_a) as the most convenient state properties.

Equation (32) may be rewritten in terms of these properties by integrating over the extent of the control volume shown in Figure 2

$$\sum_a \frac{\partial}{\partial\theta}(m_a h_a)_y = \Delta\left(kA\frac{\partial T}{\partial y}\right)_\theta + \Delta(\dot{m}_g h_g)_\theta \qquad (33)$$

where a = I, c, or r , and the differences on the right hand side are between the top and bottom of the control volume. In order to develop a practical numerical solution it is convenient to consider a coordinate system fixed to the receding surface (a moving control volume). For this purpose it is

desired to transform Equation (33), which is written for a control volume, y = constant , to an equation written for a moving coordinate system, x = constant. The storage term on the left side of Equation (33) may be related to its counterpart in the moving coordinate system in the following manner. It is noted that the mass of constituent a and its enthalpy may be expressed purely as functions of space and time.

$$m_a h_a = f(y,\theta)$$

so:

$$\frac{\partial}{\partial\theta}(m_a h_a)_x = \frac{\partial}{\partial\theta}(m_a h_a)_y + \frac{\partial}{\partial y}(m_a h_a)_\theta \left.\frac{\partial y}{\partial\theta}\right|_x \tag{34}$$

The x and y coordinates and their derivatives are related through Equations (13) and (14)

$$\left.\frac{\partial y}{\partial\theta}\right|_x = \dot{s} \tag{35}$$

Utilizing this relation and noting that differentiation with respect to x or y at constant time (θ) is equivalent,enables expressing Equation (34) in the following manner:

$$\frac{\partial}{\partial\theta}(m_a h_a)_y = \frac{\partial}{\partial\theta}(m_a h_a)_x - \dot{s}\,\frac{\partial}{\partial x}(m_a h_a)_\theta$$

Substituting the above into Equation (33) yields a subsurface energy equation in terms of the moving coordinate system.

$$\sum_a \overset{\text{I}}{\frac{\partial}{\partial\theta}(m_a h_a)_x} = \overset{\text{II}}{\Delta\left(kA\left.\frac{\partial T}{\partial x}\right|_\theta\right)} + \overset{\text{III}}{\Delta(\dot{m}_g h_g)_\theta} + \overset{\text{IV}}{\dot{s}\,\frac{\partial}{\partial x}(m_a h_a)_\theta} \tag{36}$$

Terms I and IV involve time and space derivatives of the control volume mass and enthalpy. It will be convenient for subsequent finite difference formulation to express enthalpy derivatives in terms of temperature derivatives. Also, the mass derivatives both include cross sectional area derivatives which may be eliminated. The following manipulations accomplish the desired result.

Term I will be considered first.

$$\frac{\partial}{\partial\theta}(m_a h_a)_x = m_a \left.\frac{\partial h_a}{\partial\theta}\right|_x + h_a \left.\frac{\partial m_a}{\partial\theta}\right|_x \tag{37}$$

The enthalpy for any constituent, a = I, c, or r , may be expressed in terms of its chemical and sensible parts

$$h_a = \Delta H_{f_a}^{T_r} + \int_{T_r}^{T} C_{p_a} dT \tag{38}$$

For a given constituent, $\Delta H_{f_a}^{T_r}$ = constant, so:

$$\left.\frac{\partial h_a}{\partial \theta}\right|_x = C_{p_a} \left.\frac{\partial T}{\partial \theta}\right|_x \tag{39}$$

Utilizing Equation (35) the mass derivative may be expressed as follows

$$\left.\frac{\partial m_a}{\partial \theta}\right|_x = \left.\frac{\partial m_a}{\partial \theta}\right|_y + \dot{S} \left.\frac{\partial m_a}{\partial \theta}\right|_x \tag{40}$$

Substituting Equations (39) and (40) into (37) yields the following representation for term I in the energy Equation (36).

$$\frac{\partial}{\partial \theta}(m_a h_a)_x = m_a C_{p_a} \left.\frac{\partial T}{\partial \theta}\right|_x + h_a \left[\left.\frac{\partial m_a}{\partial \theta}\right|_y + \dot{S} \left.\frac{\partial m_a}{\partial x}\right|_\theta\right] \tag{41}$$

Utilizing Equation (39), term IV in the energy Equation (36) may be written as:

$$\dot{S} \frac{\partial}{\partial x}(m_a h_a)_\theta = \dot{S} m_a C_{p_a} \left.\frac{\partial T}{\partial x}\right|_\theta + \dot{S} h_a \left.\frac{\partial m_a}{\partial x}\right|_\theta \tag{42}$$

Substitution of Equations (41) and (42) into Equation (36) yields the desired form of the subsurface energy equation for a control volume of finite extent in terms of a coordinate system fixed to the receding surface.

$$\sum_a m_a C_{p_a} \left.\frac{\partial T}{\partial \theta}\right|_x = \Delta\left(kA \left.\frac{\partial T}{\partial x}\right|_\theta\right) + \Delta(\dot{m}_g h_g)_\theta + \dot{S} \sum_a m_a C_{p_a} \left.\frac{\partial T}{\partial x}\right|_\theta + \sum_a h_a \left.\frac{\partial m_a}{\partial \theta}\right|_y \tag{43}$$

It is noted that differentiation of the last term is at constant y. It is expressed in this manner for convenience since the decomposition events (a = r) are represented at constant y, (see Eq. (22)).

In the following section a finite difference representation for the differential equations presented in this section is proposed.

SECTION 4
FINITE DIFFERENCE FORMULATION

The need for a computational scheme to mathematically model the thermochemical response of a charring material experiencing subsurface coking reactions was introduced in Section 1. In Section 2, a phenomenological model was introduced for representing the state of the charring material and its pyrolysis products, and for representing the rate at which coking reactions may proceed. Section 3 presented abbreviated derivations of the differential equations appropriate to representing the transfer of mass, momentum, and energy for the chosen phenomenological model. In this section, the equations presented above are cast into finite difference form appropriate for coding into a computational scheme.

Examination of the equations presented in Section 3 reveals that finite difference formulation of the energy conservation Equation (43) and the pressure drop relation (Eq.(29)) may be accomplished in a rather straightforward manner provided the coefficients appearing in these relations are known . The coefficients most usually contain information relating to the state of the charring material or the pyrolysis gas products. As the problem has been formulated, the state of the charring material is uniquely defined by its temperature and composition (i.e., relative quantity of each constituent; I, C, or r), and the pyrolysis gas state is defined by its pressure, temperature, and composition (i.e., $\tilde{K}_{cg}$). The composition of the charring material and the gaseous pyrolysis products is obtained from the species conservation relations. A finite difference formulation of the species conservation relations is presented first, in Section 4.1. Finite difference equations for evaluating the char layer pressure drop are presented next, in Section 4.2, and are followed, in Section 4.3, by a finite difference formulation of the subsurface energy balance. The finite difference representation of the geometrical configuration results from dividing the material into a number of discrete zones or nodes. The generalized coordinate system and nodal identification scheme is shown in Figure 4.

4.1 SPECIES CONSERVATION

In this section, the differential equations for the rate of change of composition of the charring material and the gaseous pyrolysis products are applied to a finite control volume in order to obtain algebraic equations relating the composition of the material and gas to other problem parameters.

The material composition in a control volume is defined by the masses of reactive (r), inert (I), and carbon (C) in the control volume. The elemental composition of the gaseous pyrolysis products is defined by the carbon mass fraction ($\tilde{K}_{cg}$). The material composition in the control volume will be considered first, in Section 4.1.1, and will be followed by finite difference relations for evaluating the pyrolysis gas flow rate and composition, in Section 4.1.2.

4.1.1 Material Composition

The control volume to be considered is shown in Figure 2 and is chosen such that its thickness, dx, is constant and its distance below the receding (heated) surface is constant (i.e., x = constant). The composition of the material in the control volume may change as a result of either of two events, coordinate system movement, or chemical reactions. The total rate of change of mass of a constituent in the control volume resulting from these two events is given by Equation (15):

$$\left.\frac{\partial m_a}{\partial \theta}\right)_x = \left.\frac{\partial m_a}{\partial \theta}\right)_y + \left.\frac{\partial m_a}{\partial x}\right)_\theta \dot{S} \qquad (15)$$

where a = I, C, or r. The first term on the right-hand side represents the change in mass of constituent "a" resulting from chemical reactions such as decomposition or coking. The second term represents mass change associated with coordinate system movement. Finite difference interpretation of the chemical reaction term requires that consideration be given to each particular class of chemical reactions, i.e., decomposition, coking, or reverse coking. Finite difference evaluation of this term will be treated subsequently, in Section 4.1.1.2. The second term, representing coordinate system motion, is considered first, in Section 4.1.1.1. Finally, in Section 4.1.1.3, the finite difference relations for material composition are summarized.

4.1.1.1 Material Composition Change Resulting from Coordinate System Motion

Finite difference evaluation of the convection term $(\partial m_a/\partial x)_\theta \dot{S}$ is obtained by considering a control volume of thickness δ_n and cross-sectional area A_n as shown in the sketch below.

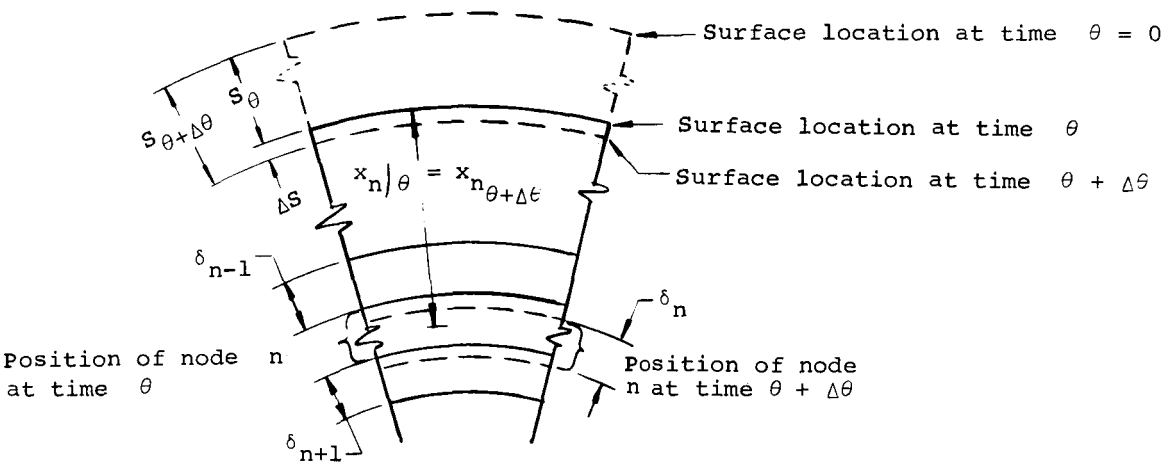

Considering each node to be of homogeneous composition, the mass change of constituent "a" in the node "n" during the interval, $\Delta\theta$, may be obtained by evaluating the mass of constituent "a" lost and gained as a result of coordinate system motion during the time interval.

$$\text{mass loss} = \left.\frac{m_a}{\delta}\right|_n \Delta S$$

$$\text{mass gain} = \left.\frac{m_a}{\delta}\right|_{n+1} \Delta S$$

The mass gain rate is obtained by taking the difference of the above and dividing by the time step, $\Delta\theta$. The following representation of the convection term results.

$$\left.\frac{\partial m_a}{\partial x}\right|_\theta \dot{S} = \left(\frac{m_{a_{n+1}}}{\delta_{n+1}} - \frac{m_{a_n}}{\delta_n}\right)\dot{S} \qquad (44)$$

It is noted that the subscript "a" refers to reactive (a = r), inert (a = I), and carbon (a = C) species. In the following section the mass change rate associated with chemical reactions is considered.

4.1.1.2 Material Composition Change Resulting from Chemical Reactions

Since the inert constituents are not allowed to react, their mass change rate due to reactions is zero, as shown by Equation (20). Finite difference representation of the mass change rate resulting from chemical reactions for reactive and carbon species may not be zero. They are treated next.

4.1.1.2.1 Reactive constituents (a = r)

The mass change rate of constituent r resulting from chemical reactions is given by Equations (22) and (23). A finite difference evaluation for the mass change rate of reactive consitutent "i" may be obtained by integrating Equation (23) over the time interval $\Delta\theta$

$$\int_{K^o_{i_\theta}}^{K^o_{i_{\theta'}}} \frac{dK^o_i}{(K^o_i)^{n_i}} = -k_i e^{-E_i/RT} \int_{\theta}^{\theta'} d\theta$$

where θ' indicates evaluation at the time $\theta + \Delta\theta$.

Evaluation of the integral obtains the following for $n_i = 1$

$$K^o_{i_{\theta'}} = K^o_{i_\theta} \exp\left[-k_i e^{-E_i/RT} \Delta\theta\right] \tag{45}$$

and, for $n_i \neq 1$

$$K^o_{i_{\theta'}} = \left[(K^o_i)^{1-n_i}_\theta - (1 - n_i) k_i e^{-E_i/RT} \Delta\theta\right]^{\frac{1}{1-n_i}} \tag{46}$$

It is noted that the above integrations were performed holding the temperature constant over the time interval. Utilization of the temperature at the "old" time, θ, results in an evaluation which is implicit in density and explicit in temperature. This method has been found to be satisfactory for a relatively wide range of materials and temperature rise rates (Ref. 1). Evaluation of the Equations (45) and (46) may be made fully implicit by utilizing the temperature at the end of the time interval, but this introduces rather severe computational complications since coupling of the decomposition and energy conservation relations is then required.

Finite difference evaluation of Equation (23) is given by:

$$\left.\frac{\partial K_i^o}{\partial \theta}\right|_y = \frac{K^o_{i_{\theta'}} - K^o_{i_\theta}}{\Delta\theta}$$

Utilizing this relation and Equation (22) enables forming an expression for the mass change rate of a reactive constituent, i, in the node "n".

$$\left.\frac{\partial m_{in}}{\partial \theta}\right|_y = \frac{m_{io}}{\Delta\theta}\left(K^o_{i_{\theta'}} - K^o_{i_\theta}\right) \tag{47}$$

where $K^o_{i_{\theta'}}$ is evaluated from Equations (45) and (46) for the reaction order, $n_i = 1.0$ and $n_i \neq 1.0$, respectively.

Finite difference formulation of the mass change rate of carbon content for each node is presented in the next section.

4.1.1.2.2 Carbon (a = c)

The carbon content in a node may change as a result of char formation reactions described above, as a result of precipitation of carbon from the gas (coking), or as a result of erosion of the char by the pyrolysis gas (reverse coking). Finite difference relations for evaluating the change in carbon content of a node resulting from each of these reactions are presented in the following three subsections.

4.1.1.2.2.1 Decomposition of reactive constituents

The rate of change of carbon mass in a node as a result of decomposition of reactive constituents is given by Equation (25)

$$\left.\frac{\partial m_c}{\partial \theta}\right|_{Decom.} = \sum_{i=1,2,3} -K^o_{c_{if}} m_{io} \left.\frac{\partial K_i^o}{\partial \theta}\right|_y \tag{25}$$

where subscript Decom. refers to the carbon change as a result of decomposition alone. Employing the same finite difference representation for the decomposition rate as before (Eq. (47)), the carbon mass change rate in the node resulting from decomposition is given by:

$$\left.\frac{\partial m_c}{\partial \theta}\right|_{n,Decom.} = \sum_{i=1,2,3} -K^o_{c_{if}} \frac{m_{io}}{\Delta\theta}\left(K^o_{i_{\theta'}} - K^o_{i_\theta}\right) \tag{48}$$

where, as before, $K^{o}_{i_\theta}$, is given by Equations (45) and (46) for $n_i = 1.0$ and $n_i \neq 1.0$, respectively. The carbon change rate resulting from forward coking reactions is considered next.

4.1.1.2.2.2 Forward coking reactions

Equation (26) relates the pyrolysis gas carbon content change rate as a result of forward coking reactions to local pressure, temperature, and gas composition.

$$\left.\frac{\partial \tilde{K}_{cg}}{\partial \theta}\right|_{coke} = - k_c e^{-E_c/RT} (P)^{n_c} (\tilde{K}_{cg} - \tilde{K}_{cgE})^{n_c} \tag{26}$$

This equation will be integrated over the extent of the node n, in order to relate the gas composition change rate to the carbon precipitation rate on the node.

$$\int_{\tilde{K}_{cg\theta}}^{\tilde{K}_{cg,\theta+\tau}} \frac{d\tilde{K}_{cg}}{(\tilde{K}_{cg} - \tilde{K}_{cgE})^{n_c}} = \int_{\theta}^{\theta+\tau} - k_c e^{-E_c/RT} P^{n_c} d\theta \tag{49}$$

where integration is performed over the thickness of the node and τ represents the transit time for the gas to pass from the bottom to the top of the node. The pressure and temperature are treated as constant throughout the node so the equilibrium gas composition, $\tilde{K}_{cgE}$, may be treated as constant over the integration interval as well. For the reaction order different from unity ($n_c \neq 1$), integration of Equation (49) yields:

$$\tilde{K}_{cg,\theta+\tau} = \tilde{K}_{cgE} + \left[(\tilde{K}_{cg\theta} - \tilde{K}_{cgE})^{1-n_c} - (1 - n_c) k_c e^{-E_c/RT} P^{n_c} \tau \right]^{\frac{1}{1-n_c}} \tag{50}$$

The carbon content of the gas entering the node, $\tilde{K}_{cg\theta}$, will be represented by the gas composition of the gas leaving the previous node, n + 1.

$$\tilde{K}_{cg\theta} = \tilde{K}_{cg,n+1} \tag{51}$$

Similarly, the carbon content of the gas leaving the node, $\tilde{K}_{cg,\theta+\tau}$, is identified with the node, n.

$$\tilde{K}_{cg,\theta+\tau} \equiv \tilde{K}_{cgn} \tag{52}$$

The transit time for the gas to pass through the node, τ, is related to the gas velocity and the nodal thickness

$$\tau = \frac{\delta}{u_g} \tag{53}$$

where u_g is the actual gas velocity passing through the node and is not to be confused with the superficial velocity (v) employed for pressure drop calculations (Eq. (29)). The actual gas velocity is related to the gas flow rate through the node as follows:

$$u_g = \frac{\dot{m}_g}{\rho_g \epsilon A} \tag{54}$$

where ρ_g is the pyrolysis gas density, ϵ is the interconnected void volume porosity, and A is the local cross-sectional area parallel to the heated surface. Utilizing Equations (53), (54), and the gas state relation,

$$\tau = \frac{P\delta M_g \epsilon A}{RT\dot{m}_g} \tag{55}$$

where R = universal gas constant and M_g = local pyrolysis gas molecular weight. Substitution of Equation (55) into (50) results in an expression for the pyrolysis gas carbon content leaving the node in the presence of forward coking reactions.

$$\left.\tilde{K}_{cg_n}\right|_{coke} = \tilde{K}_{cgE_n} + \left[(\tilde{K}_{cg_{n+1}} - \tilde{K}_{cgE_n})^{1-n_c} - (1 - n_c) k_c e^{-E_c/RT_n} P_n^{n_c+1} \frac{\delta_n M_{g_n} \epsilon_n A_n}{RT_n \dot{m}_{g_{n+1}}} \right]^{\frac{1}{1-n_c}} \tag{56}$$

where the subscript coke signifies the gas composition leaving node n as a result of coking reactions alone. It is noted that this term must be modified if the node is decomposing at the same time it is receiving carbon from the gas. Evaluation of the gas composition including all effects is treated subsequently, in Section 4.1.2. Equation (56) is valid for a non-unity reaction order, $n_c \neq 1.0$. For $n_c = 1.0$, integration of Equation (49) and utilization of Equation (55) yields

$$\tilde{K}_{cg_n}\Big|_{coke} = \tilde{K}_{cgE_n} + (\tilde{K}_{cg_{n+1}} - \tilde{K}_{cgE_n}) \exp\left[- k_c e^{-E_c/RT} p^2 \frac{\delta_n M_{g_n} \epsilon_n A_n}{RT_n \dot{m}_{g_{n+1}}} \right] \tag{57}$$

Equations (56) and (57) represent the carbon content of the gas leaving the node which would result from forward coking reactions alone for reaction orders (n_c) of non-unity and unity, respectively.

The purpose of this section is to obtain finite difference expressions for the carbon content change rate of a node resulting from forward coking reactions. This is accomplished by integrating Equation (17) over the node and employing Equations (56) and (57) to represent the gas composition. Equation (17) relates the gas composition change rate to the char material composition change rate.

$$\frac{\partial}{\partial y} (\tilde{K}_{cg} \dot{m}_g)_\theta = \frac{\partial}{\partial \theta} (\tilde{K}_c \rho A)_y \tag{17}$$

Rewriting Equation (17) yields

$$\dot{m}_g \frac{\partial \tilde{K}_{cg}}{\partial y}\Big|_\theta + \tilde{K}_{cg} \frac{\partial \dot{m}_g}{\partial y}\Big|_\theta = \frac{\partial}{\partial \theta} (\tilde{K}_c \rho A)_y \tag{58}$$

The first term represents gas composition change as results, for example, from coking reactions. The second term represents pyrolysis gas flow rate change as results from decomposition of reactive constituents. The latter effect was treated above (Eq. (25)). At this point it is most convenient to consider the char carbon content change associated with coking reactions alone, and, for this purpose the second term may be ignored. Integration of Equation (58) then obtains

$$\int_{\tilde{K}_{cg_{n+1}}}^{\tilde{K}_{cg_n}} \dot{m}_g d\tilde{K}_{cg} = \int_{y_n + \frac{\delta_n}{2}}^{y_n - \frac{\delta_n}{2}} (\tilde{K}_c \rho A)_y dy \qquad (59)$$

where the integration is performed over the interval from the bottom to the top of node n. The integral on the right represents the time rate of change of carbon content in the node n as a result of coking reactions. Performing the integration yields:

$$\left.\frac{\partial m_c}{\partial \theta}\right)_{n,coke} = \dot{m}_{g_{n+1}} \left[\tilde{K}_{cg_{n+1}} - \left. \tilde{K}_{cg_n} \right)_{coke} \right] \qquad (60)$$

where the subscript "coke" signifies the change resulting from coking alone, and $\dot{m}_{g_{n+1}}$ is the pyrolysis gas flow rate entering the node n (leaving node n+1). Similarly, $\tilde{K}_{cg_{n+1}}$ represents the composition of the gas entering node n. The mass fraction of carbon in the gas leaving node n due to coking alone, $\left. \tilde{K}_{cg_n} \right)_{coke}$ is evaluated by either Equations (56) or (57) depending on the reaction order for coking (n_c).

The mass change rate of carbon in a node resulting from erosion by the pyrolysis gas (reverse coking) is considered next.

4.1.1.2.2.3 Reverse coking reactions

The pyrolysis gas composition change between two adjacent nodes resulting from reverse coking reactions is obtained by direct integration of Equation (28) which yields:

$$\tilde{K}_{cg_n} - \tilde{K}_{cg_{n+1}} = (\tilde{K}_{cgE_n} - \tilde{K}_{cgE_{n+1}}) \qquad (61)$$

where the equilibrium pyrolysis gas carbon content, $\tilde{K}_{cgE}$, is evaluated at the local temperature and pressure of the designated nodes. Substitution of the above into Equation (60) yields the desired expression for reverse coking reactions.

$$\left.\frac{\partial m_c}{\partial \theta}\right)_{n,coke} = (\tilde{K}_{cg_{n+1}} - \tilde{K}_{cgE_n}) \qquad (62)$$

It is noted that Equation (62) is identical to Equation (60) with the exception that the quantity $\tilde{K}_{cg_n}\big|_{coke}$ is now replaced with $\tilde{K}_{cgE_n}$. It will be most convenient to employ Equation (60) in both events with the interpretation that the quantity $\tilde{K}_{cg_n}\big|_{coke}$ represents the elemental carbon mass fraction in the gas leaving the node n in the presence of coking reactions (forward, or reverse), but not considering the effect of decomposition of reactive constituents in the node n. For forward coking reactions, $(\tilde{K}_{cg_{n+1}} - \tilde{K}_{cgE_n}) > 0$, Equations (56) or (57) are employed to evaluate $\tilde{K}_{cg_n}\big|_{coke}$ depending upon the coking reaction order, and for reverse coking, $(\tilde{K}_{cg_{n+1}} - \tilde{K}_{cgE_n}) \leqq 0$, $\tilde{K}_{cg_n}\big|_{coke} = \tilde{K}_{cgE_n}$.

4.1.1.3 Summary of Relations for Evaluating Material Composition

The finite difference relations developed in this section are summarized and combined here. This is accomplished by considering the net change in composition of a node resulting from all events taken collectively. Algebraic equations for the mass of each constituent at the end of a time step, $\Delta\theta$, are given in terms of conditions at the beginning of the time step. Inert, reactive, and carbon constituents are considered first, in Sections 4.1.1.3.1 through 4.1.1.3.3, and are followed in Section 4.1.1.3.4, by relations for the total nodal mass.

4.1.1.3.1 Inert constituents (a = I)

Combining Equations (15) and (20) for inert constituents (a = I) yields

$$\left.\frac{\partial m_I}{\partial \theta}\right)_x = \left.\frac{\partial m_I}{\partial x}\right)_\theta \dot{S} \tag{63}$$

Utilizing Equation (44) to represent the right-hand side and expressing in finite difference form obtains:

$$\frac{m_{I_{n\theta'}} - m_{I_{n\theta}}}{\Delta\theta} = \left(\frac{m_{I_{n+1}}}{\delta_{n+1}} - \frac{m_{I_n}}{\delta_n}\right)\dot{S} \tag{64}$$

where it is recalled that $\theta' = \theta + \Delta\theta$. Rearranging yields the desired relation for the mass of inert constituent in a node at the end of the time interval.

$$m_{I_{n\theta'}} = m_{I_{n\theta}} + \left(\frac{m_{I_{n+1}}}{\delta_{n+1}} - \frac{m_{I_n}}{\delta_n}\right)\dot{S}\Delta\theta \tag{65}$$

4.1.1.3.2 Reactive constituents (a = r)

The mass of reactive (decomposable) constituents in a node at the end of a time step depends upon the amount of decomposition and convection resulting from coordinate system motion. Substitution of Equations (44), (45) and (47) into Equation (15) yields the finite difference expression for a reactive constituent with reaction order of unity

$$\frac{m_{i_{n\theta'}} - m_{i_{n\theta}}}{\Delta\theta} = \left(\frac{m_{i_{n+1}}}{\delta_{n+1}} - \frac{m_{i_n}}{\delta_n}\right)\dot{S} - \frac{m_{i_o}}{\Delta\theta} K^o_{i_\theta}\left[1 + \exp\left(k_i e^{-E_i/RT}\Delta\theta\right)\right] \quad (66)$$

The mass of constituent i in the node at the end of the time interval is then given by:

$$m_{i_{n\theta'}} = m_{i_{n\theta}} + \left(\frac{m_{i_{n+1}}}{\delta_{n+1}} - \frac{m_{i_n}}{\delta_n}\right)\dot{S}\Delta\theta - m_{i_o} K^o_{i_\theta}\left[1 + \exp\left(k_i e^{-E_i/RT}\Delta\theta\right)\right] \quad (67)$$

The above equation is for reactive constituents having a unity reaction order ($n_i = 1.0$). Similarly, for constituents having non-unity reaction order, Equations (15), (44), (46), and (47) yield:

$$m_{i_{n\theta'}} = m_{i_{n\theta}} + \left(\frac{m_{i_{n+1}}}{\delta_{n+1}} - \frac{m_{i_n}}{\delta_n}\right)\dot{S}\Delta\theta - m_{i_o}\left\{K^o_{i_\theta} - \left[\left(K^o_{i_\theta}\right)^{1-n_i} - (1 - n_i)k_i e^{-E_i/RT}\Delta\theta\right]^{\frac{1}{1-n_i}}\right\} \quad (68)$$

The total mass of reactive constituents in a node is given by:

$$m_{r_{n\theta'}} = \sum_{i=1,2,3} m_{i_{n\theta'}} \quad (69)$$

4.1.1.3.3 Carbon constituents (a = c)

The mass of carbon in a node at the end of the time step depends upon the magnitudes of convection, decomposition, and coking. Utilizing Equation (15), (44), (48), and (60) obtains

$$m_{c_{n\theta'}} = m_{c_{n\theta}} + \left(\frac{m_{c_{n+1}}}{\delta_{n+1}} - \frac{m_{c_n}}{\delta_n} \right) \dot{S} \Delta\theta + \sum_{i=1,2,3} K^o_{c_{if}} m_{i_o} (K^o_{i_\theta} - K^o_{i_{\theta'}})$$

$$+ \dot{m}_{g_{n+1}} \left[\tilde{K}_{cg_{n+1}} - \tilde{K}_{cg_n}\Big|_{coke} \right] \Delta\theta \qquad (70)$$

The terms $K^o_{i_{\theta'}}$ and $\tilde{K}_{cg_n}\Big|_{coke}$ are subject to several interpretations as follows. For a decomposable constituent, i, having a reaction order of unity, $K^o_{i_{\theta'}}$, is given by Equation (45)

$$K^o_{i_{\theta'}} = K^o_{i_\theta} \exp \left[- k_i e^{-E_i/RT} \Delta\theta \right] \qquad (45)$$

and, for non-unity reaction order, Equation (46) is employed.

$$K^o_{i_{\theta'}} = \left[\left(K^o_i \right)^{1-n_i}_{\theta} - (1 - n_i) k_i e^{-E_i/RT} \Delta\theta \right]^{\frac{1}{1-n_i}} \qquad (46)$$

The following interpretations apply to the quantity $\tilde{K}_{cg_n}\Big|_{coke}$

For $(\tilde{K}_{cg_{n+1}} - \tilde{K}_{cgE_n}) > 0$

and $n_c = 1.0$

$$\tilde{K}_{cg_n} = \tilde{K}_{cgE_n} + (\tilde{K}_{cg_{n+1}} - \tilde{K}_{cgE_n}) \exp \left[- k_c e^{-E_c/RT} P^2 \frac{\delta_n M_{g_n} \epsilon_n A_n}{RT_n \dot{m}_{g_{n+1}}} \right] \qquad (57)$$

For $(\tilde{K}_{cg_{n+1}} - \tilde{K}_{cgE_n}) > 0$

and $n_c \neq 1.0$

$$\tilde{K}_{cg_n} = \tilde{K}_{cgE_n} + \left[(\tilde{K}_{cg_{n+1}} - \tilde{K}_{cgE_n})^{1-n_c} \right.$$

$$\left. - (1 - n_c) k_c e^{-E_c/RT} P_n^{n_c+1} \frac{\delta_n M_{g_n} \epsilon_n A_n}{RT_n \dot{m}_{g_{n+1}}} \right]^{\frac{1}{1-n_c}} \qquad (56)$$

Equations (56) and (57) represent forward coking reactions. Reverse coking reactions will occur when $(\tilde{K}_{cg_{n+1}} - \tilde{K}_{cgE_n}) = 0$, and for this case $\tilde{K}_{cg_n}\big|_{coke} = \tilde{K}_{cgE_n}$.

It is noted that the equations presented thus far in this summary section are sufficient for representing the material composition for solution of the pressure-drop and energy conservation relations to be presented subsequently. Several quantities relative to material composition and density, in addition to those presented thus far, are of interest and are described in the following subsection.

4.1.1.3.4 Total nodal mass

The total mass of a node is given by Equation (10)

$$m_n = \sum_a m_{a_n} \tag{10}$$

where a = I, r, and c. The masses of inert, reactive, and carbon constituents in a node are given by Equations (65), (69), and (70), respectively. As a matter of convenience in interpreting computer program output it is appropriate that material composition be given in terms of intensive rather than extensive properties. The definition of nodal mass fractions and nodal density accomplish this purpose.

$$K_{a_n} = \frac{m_{a_n}}{m_n} \tag{71}$$

for a = I, r, or c, and the nodal density is given by

$$\rho_n = \frac{m_n}{A_n \delta_n} \tag{72}$$

4.1.2 Pyrolysis Gas Composition

In this section, finite difference relations for pyrolysis gas composition and flow rate are presented. Most of the fundamental relations required for characterizing the pyrolysis gas composition and flow rate were developed above in Section 4.1.1, and, as such, the development in this section is relatively straightforward.

The gas flow rate leaving a node, n, may be related to the gas flow rate entering the node and the gas generation rate in the node by integrating

Equation (19) over a nodal volume.

$$\int_{\dot{m}_{g_{n+1}}}^{\dot{m}_{g_n}} d\dot{m}_g = \int_{y_n+\delta_n/2}^{y_n-\delta_n/2} \frac{\partial}{\partial\theta} (\rho A)_y \tag{73}$$

From which:

$$\dot{m}_{g_n} = \dot{m}_{g_{n+1}} + \left.\frac{\partial m_n}{\partial\theta}\right)_y \tag{74}$$

It is noted that differentiation of the nodal mass is performed at constant y, and therefore includes only the nodal mass change rate associated with chemical reactions. These chemical reactions may consist of gas generation resulting from decomposition, or mass transfer resulting from coking reactions.

$$\left.\frac{\partial m_n}{\partial\theta}\right)_y = \sum_{i=1,2,3} \left.\frac{\partial m_{i_n}}{\partial\theta}\right)_y + \left.\frac{\partial m_{c_n}}{\partial\theta}\right)_y \tag{75}$$

Substituting Equations (47), (48), and (60) into the above yields;

$$\dot{m}_{g_n} = \dot{m}_{g_{n+1}} + \sum_{i=1,2,3} \frac{m_{i_o}}{\Delta\theta} (1 - K^o_{c_{if}}) (K^o_{i_{\theta'}} - K^o_{i_\theta})_n$$

$$+ \dot{m}_{g_{n+1}} \left[\tilde{K}_{cg_{n+1}} - \tilde{K}_{cg_n}\Big|_{coke} \right] \tag{76}$$

where, as before, $K^o_{i_{\theta'}}$ is given by Equations (45) or (46) depending on reaction order, and $\tilde{K}_{cg_n}\big|_{coke}$ is given by either Equations (56) and (57) for forward coking, or $\tilde{K}_{cg_n}\big|_{coke} = \tilde{K}_{cgE_n}$ for reverse coking.

The elemental carbon content in the pyrolysis gas, $\tilde{K}_{cg}$, may be obtained in a number of ways. Perhaps the most straightforward approach is to consider the elemental carbon contribution of each of the terms in Equation (76). The gas leaving the node n, has a carbon content, $\tilde{K}_{cg_n}$, and the gas entering

has a carbon content $\tilde{K}_{cg_{n+1}}$. The second term on the right side of equation (76) represents the gas generated in the node as a result of organic decomposition reactions. The carbon content of the gas is designated by

$$\tilde{K}_{cg_{io}} = \frac{(K^o_{c_i} - K^o_{c_{if}})}{(1 - K^o_{c_{if}})} \frac{\text{Lb carbon in gas}}{\text{Lb gas generated}} \tag{77}$$

The last term in Equation (76) represents coking. The mass transfer associated with coking is pure carbon by definition. Utilizing the above definitions, Equation (76), and performing an elemental carbon balance on the gas results in an equation for the elemental carbon content of the gas leaving the node, n.

$$\tilde{K}_{cg_n} = \frac{2\tilde{K}_{cg_{n+1}} \dot{m}_{g_{n+1}} + \sum_{i=1,2,3} (K^o_{c_i} - K^o_{c_{if}}) \frac{m_{i_o}}{\Delta\theta} (K^o_{i_{\theta'}} - K^o_{i_\theta})_n}{\dot{m}_{g_n}}$$

$$- \frac{\dot{m}_{g_{n+1}}}{\dot{m}_{g_n}} K_{cg_n}\Big)_{coke} \tag{78}$$

4.2 CHAR LAYER PRESSURE DROP

It is desired to cast the pressure drop correlation Equation (29) into a form including only variables which are readily available from the computation scheme for solving the mass and energy conservation equations.

The velocity of the gas passing through the porous char is related to the gas flow rate per unit area by Equation (30). Introducing the gas state equation ($P = \rho_g RT/M_g$) into Equation (30) yields:

$$v = \frac{\dot{m}_g}{PM_g A} RT \tag{79}$$

It is convenient to define a viscosity law for the pyrolysis gas

$$\mu = \mu_o \left(\frac{T}{T_o}\right)^n \tag{80}$$

where μ_o and T_o represent a reference viscosity and reference temperature.

Substituting Equations (79) and (80) in (29) yields the following relation for a linear pressure drop across a node, n.

$$\left(\frac{dP}{dy}\right)_n = \left[\alpha\mu_o \left(\frac{T}{T_o}\right)^n + \beta \frac{\dot{m}_g}{A}\right]_n \left(\frac{\dot{m}_g RT}{PM_g A}\right)_n \tag{81}$$

where the coefficients α, β, are functions of the local char permeability. The pressure at the top of node 1 (the heated surface node) is taken equal to the prescribed boundary layer edge pressure ($P_1 = P_e$). The pressure at the top of any other node is related to the pressure drop across and pressure at the top of the node above it.

$$P_n = P_{n-1} + \left(\frac{dP}{dy}\right)_{n-1} \delta_{n-1} \tag{82}$$

or

$$P_n = P_e + \sum_{i=1}^{n-1} \left(\frac{dP}{dy}\right)_i \delta_i \tag{83}$$

The computation may be performed in an explicit manner, that is, after obtaining solutions of the energy and mass conservation equations, a single pass through the nodal network from heated surface (n = 1) to the virgin material yields the pressure distribution entirely in terms of conditions existing at the end of the previous time step. The solution corresponds to assuming an impermeable boundary condition at the rear face of the ablative material. The summation is performed just to the virgin material since below this point, $\dot{m}_g = 0$.

4.3 ENERGY CONSERVATION

A modified differential formulation of the subsurface energy conservation equation was developed above, in Section 3.3, and is represented by Equation (43).

$$\sum_a m_a C_{p_a} \left(\frac{\partial T}{\partial \theta}\right)_x = \Delta \left(kA \frac{\partial T}{\partial x}\right)_\theta + \Delta(\dot{m}_g h_g)_\theta + \dot{S} \sum_a m_a C_{p_a} \left(\frac{\partial T}{\partial x}\right)_\theta + \sum_a h_a \left(\frac{\partial m_a}{\partial \theta}\right)_y \tag{43}$$

Finite difference formulation of Equation (43) is relatively straightforward. The primary features which distinguish between various possible formulations

are associated with whether an implicit or explicit solution is desired. Finite difference formulations corresponding to solutions which are explicit and implicit with respect to temperature are given here.

Based upon the satisfactory accuracy checks for the forward difference formulation presented in Reference 1, the same basic differencing philosophy is adopted here, and results in the following finite difference interpretation for Equation (43).

$$T_{n_{\theta'}} = T_{n_\theta} + \frac{\Delta\theta}{\sum_{a=I,c,r} \left(m_a C_{p_a}\right)_n} \left\{ \frac{(T_{n-1} - T_n)_\theta}{\frac{\delta_{n-1}}{2k_{n-1}A_{n-1}} + \frac{\delta_n}{2k_nA_n}} \right.$$

$$- \frac{(T_n - T_{n+1})_\theta}{\frac{\delta_n}{2k_nA_n} + \frac{\delta_{n+1}}{2k_nA_n}} + (\dot{m}_g h_g)_{n+1} - (\dot{m}_g h_g)_n$$

$$\left. + \sum_{a=c,r} h_{a_n} \left.\frac{\partial m_a}{\partial\theta}\right|_y \right\} + \dot{S} \left[\frac{T_{n+1} - T_n}{(\delta_{n+1} + \delta_n)/2} \right] \Delta\theta \qquad (84)$$

where

$$\sum_{a=c,r} \left.\frac{\partial m_a}{\partial\theta}\right|_y = \left.\frac{\partial m_c}{\partial\theta}\right|_{y,\text{decom}} + \left.\frac{\partial m_c}{\partial\theta}\right|_{\text{coke}} + \left.\frac{\partial m_r}{\partial\theta}\right|_y \qquad (85)$$

$\left.\frac{\partial m_c}{\partial\theta}\right|_{y,\text{decom}}$ is given by Equation (48)

$\left.\frac{\partial m_c}{\partial\theta}\right|_{\text{coke}}$ is given by Equation (60)

$$\left.\frac{\partial m_r}{\partial\theta}\right|_y = \sum_{i=1,2,3} \left.\frac{\partial m_i}{\partial\theta}\right|_y$$

and $\left.\frac{\partial m_i}{\partial\theta}\right|_y$ is given by Equation (47)

The enthalpy of constituent, a, is given by:

$$h_{a_n} = \Delta H_{f_a}^{T_r} + \int_{T_r}^{T_n} C_{p_a} dT \tag{86}$$

The mass fraction is given by Equation (71)

$$K_{a_n} = \frac{m_{a_n}}{m_a} \tag{71}$$

The heat of formation of constituent a, $\Delta H_{f_a}^{T_r}$ is an input constant and the specific heat, C_{p_a}, is a function of temperature alone. The pyrolysis gas flow rate, $\dot{m}_g$, is given by Equation (76), and the pyrolysis gas enthalpy, h_g, is considered to be a function of temperature, pressure, and elemental carbon content, $\tilde{K}_{c_g}$. Various models may be employed to represent the pyrolysis gas enthalpy, as for example that described earlier in Section 2. Whatever model is selected to represent the pyrolysis gas molecular configuration, and hence its enthalpy at a given temperature, it would seem that the parameters, P, T, and $\tilde{K}_{c_g}$ will be required to characterize the pyrolysis gas enthalpy. Selection of a model to represent the thermal conductivity in the charring material has not been given detailed consideration. Cursory examination suggests that the primary factors to be considered in characterizing the thermal conductivity would be the relative mass of each constituent, K_a, the porosity, and the temperature. Such a model has been postulated and verified to a certain extent (Ref. 9) for partially degraded organic reinforced ablative materials. The same fundamental approach may yield realistic correlations for "coked" chars as well. Evaluation of the remainder of the terms in the energy Equation (84) is apparent from an examination of the geometrical configuration being analyzed (Fig. 2) and the nomenclature list.

Implicit formulation of the energy equation is most conveniently accomplished in the same manner as reported in Reference 1 by linearizing the nonlinear terms. The following relation is obtained.

$$T_{n_{\theta'}} = T_{n_\theta} + \frac{\Delta\theta}{\sum_{a=I,c,r} \left(m_a C_{p_a}\right)_{n,\theta}} \left\{ \frac{\left(T_{n-1} - T_n\right)_{\theta'}}{\frac{\delta_{n-1}}{2k_{n-1}A_{n-1}} + \frac{\delta_n}{2k_nA_n}} - \frac{\left(T_n - T_{n+1}\right)_{\theta'}}{\frac{\delta_n}{2k_nA_n} + \frac{\delta_{n+1}}{2k_{n+1}A_{n+1}}} \right.$$

(Equation continued on following page)

(Equation continued from preceding page)

$$+ \dot{m}_{g_{n+1,\theta}} \left[h_{g_{n+1,\theta}} + C_{p_{g_{n,\theta}}} (T_{n+1,\theta'} - T_{n+1,\theta}) \right]$$

$$- \dot{m}_{g_{n,\theta}} \left[h_{g_{n,\theta}} + C_{p_{g_{n,\theta}}} (T_{n,\theta'} - T_{n,\theta} \right] + \sum_{a=c,r} \left[h_{a_{n,\theta}} \right.$$

$$\left. + C_{p_{a_{n,\theta}}} (T_{n,\theta'} - T_{n,\theta} \right] \left. \frac{\partial m_a}{\partial \theta} \right|_y + \dot{S} \Delta\theta \left[\frac{T_{n+1,\theta'} - T_{n,\theta'}}{(\delta_{n+1} + \delta_n)/2} \right] \qquad (87)$$

The specific heats appearing in Equation (87) may be evaluated directly from an input tabulation for the material, C_{p_a}, and, for the gas, the specific heat is obtained by numerically differentiating the input gas enthalpy data for the temperature and pressure at the node, n. Equation (87) is implicit in temperature and explicit in mass, that is, the mass transfer events, which are temperature dependent, are evaluated at the "old" temperature (at θ). This type of treatment has been found to be quite satisfactory for numerical characterization of straight decomposing materials. It is difficult to assess the adequacy of this type of formulation for the problem being considered here since the kinetic coefficients for characterizing the coking reactions are not presently in hand.

Equations (84) and (87) are appropriate for all nodes in the ablation material except the heated surface node, n = 1. Treatment of the heated surface boundary condition may be accomplished in the same manner as described in Reference 1 where it is shown that the surface (char) mass recession rate may be related to the surface temperature, surface pressure, pyrolysis off-gas rate, and boundary layer mass transfer coefficient.

$$B'_c = f(P_e, T_e, B'_g)$$

where $B'_c = \dot{m}_c / \rho_e u_e C_M A$, $B'_g = \dot{m}_g / \rho_e u_e C_M A$. In the present analysis, one additional parameter is needed, the pyrolysis gas composition, which may be represented by the pyrolysis gas elemental carbon content.

$$B'_c = f(P_e, T_e, B'_g, \tilde{K}_{c_g})$$

Exept for this difference, the surface boundary condition evaluation may be treated in the same manner as described in Reference 1.

SECTION 5
SUMMARY AND CONCLUSION

The probable importance of subsurface coking reactions has been identified and a phenomenological model to represent energy, mass, and momentum transfer events in a charring ablation material undergoing coking reactions has been postulated. Differential equations were developed to represent a mathematical analog of the phenomenological model and the equations were cast into finite difference form suitable for coding into a computational scheme.

The phenomenological model is based upon a certain amount of conjecture because sufficient quantitative experimental observations to construct a rigorous model do not presently exist. Part of the motivation behind conducting the study presented herein has been a desire to identify the parameters and groups of parameters which require experimental evaluation, since, ideally the parameters which are controlled and measured in an experiment may be directly related to the parameters required as input to a computational scheme. The phenomenological model presented herein is believed reasonable and the finite difference representation is believed appropriate for developing an efficient computational scheme.

REFERENCES

1. Moyer, C. B., and Rindal, R. A.: Finite Difference Solution for the In-depth Response of Charring Materials Considering Surface Chemical and Energy Balances. Aerotherm Report No. 66-7, Part II, March 14, 1967

2. Kratsch, K. M., Hearne, L. F., and McChesney, H. R.: Thermal Performance of Heat Shield Composites During Planetary Entry. Lockheed Missiles and Space Company, Sunnyvale, Calif., Report LMSC-803099, October 1963.

3. Quinville, J. A., and Solomon, J.: Ablating Body Heat Transfer. Aerospace Corp., El Segundo, Calif., SSD-TDR-63-159 (AD 429 198), January 15, 1964.

4. Wells, P. B.: A Method for Predicting the Thermal Response of Charring Ablation Materials. Boeing Co., Seattle, Wash., Report D2-23256 (AD-443 144), July 1964.

5. Personal communication, D. M. Curry, NASA Manned Spacecraft Center, Houston, Texas.

6. Schaefer, J. W.: A Study of Composite Material Chunking Mechanisms. Vidya Progress Report, Aerojet-General P.O. No. 450342-0800, January 31, 1965.

7. Friedman, H. L.: The Products of Flash Pyrolysis of Phenyl-Formaldehyde by Time-of-Flight Mass Spectroscopy. General Electric Report R62SD81, September 1962.

8. Green, L. Jr.: Heat, Mass, and Momentum Transfer in Flow Through Proous Media. ASME-AIChE Heat-Transfer Conference, August 11-15, 1957.

9. Rindal, R. A., Flood, D. T., and Clark, K. J.: Experimental and Theoretical Analysis of Ablative Material Response in a Liquid-Propellant Rocket Engine. Third Quarterly Progress Report, Aerotherm Contract 7003, June 30, 1966.

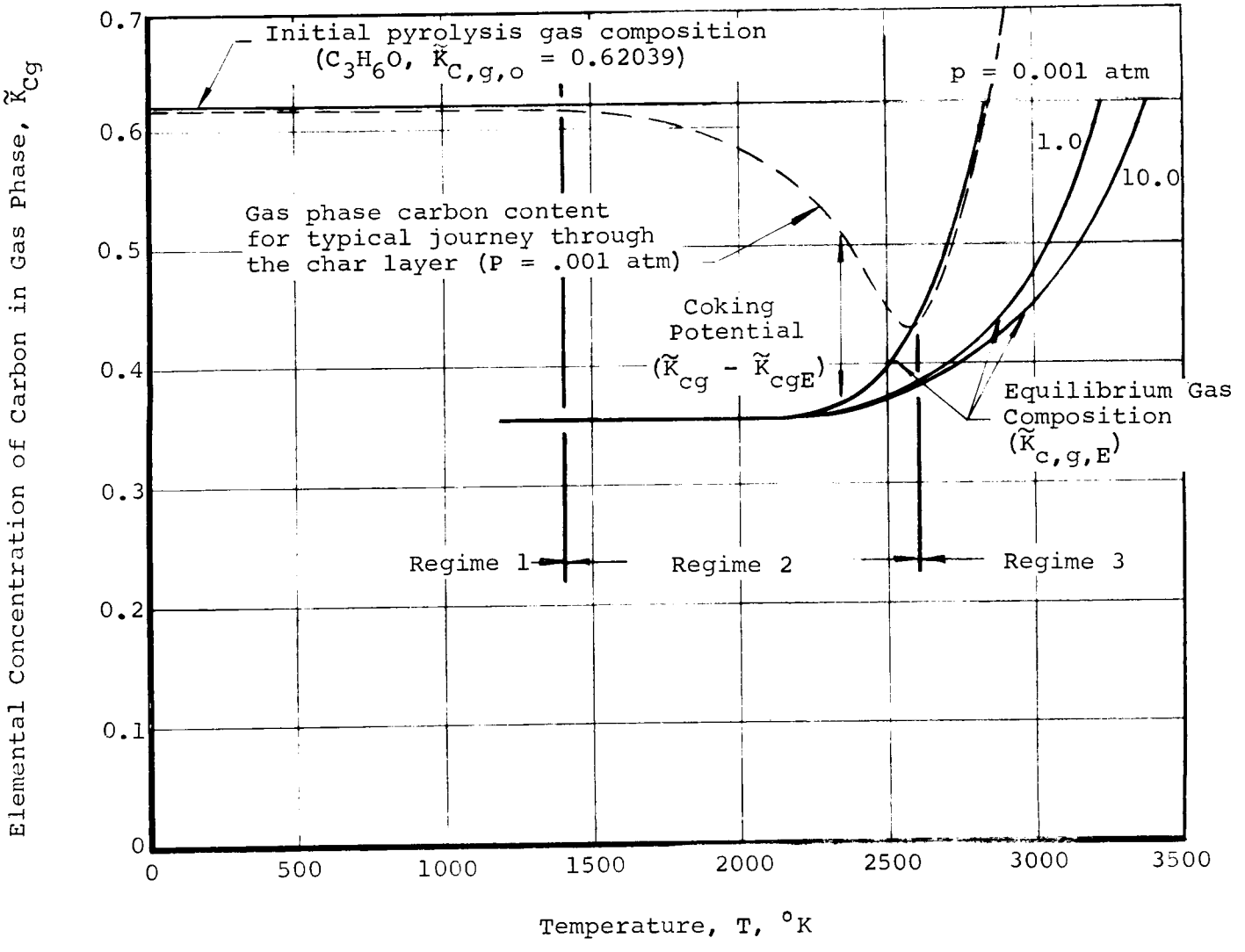

Figure 1. Gas Phase Elemental Carbon Concentration and Coking Potential for Typical Phenolic Pyrolysis Gas

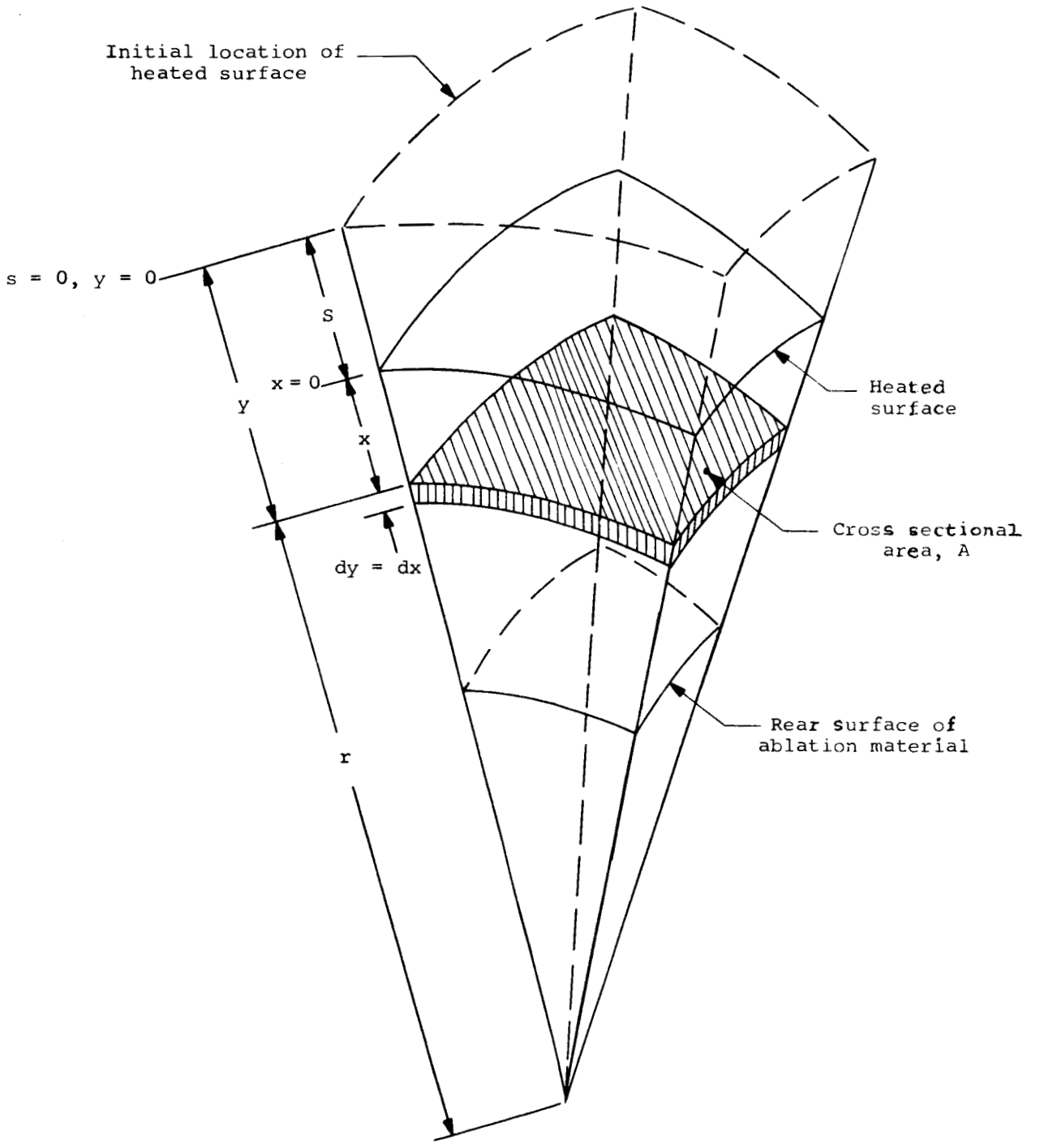

Figure 2. Geometrical Configuration and Coordinate System Illustration

$$\frac{dP}{dy} = \alpha\mu v + \beta\rho v^2$$

Note: $\alpha_o = 1\ ft^{-2}$

$\beta_o = 1\ ft^{-1}$

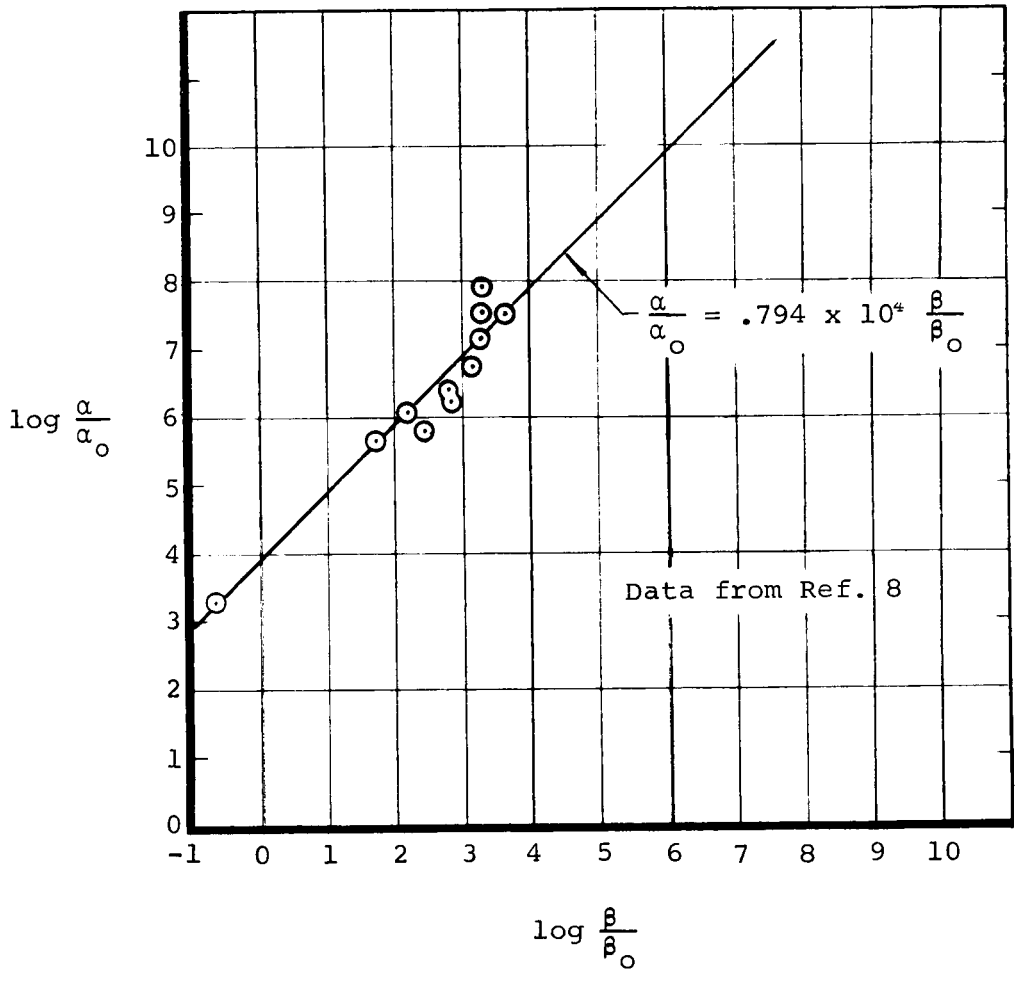

Figure 3. Experimentally Determined Coefficients for Flow through Porous Media

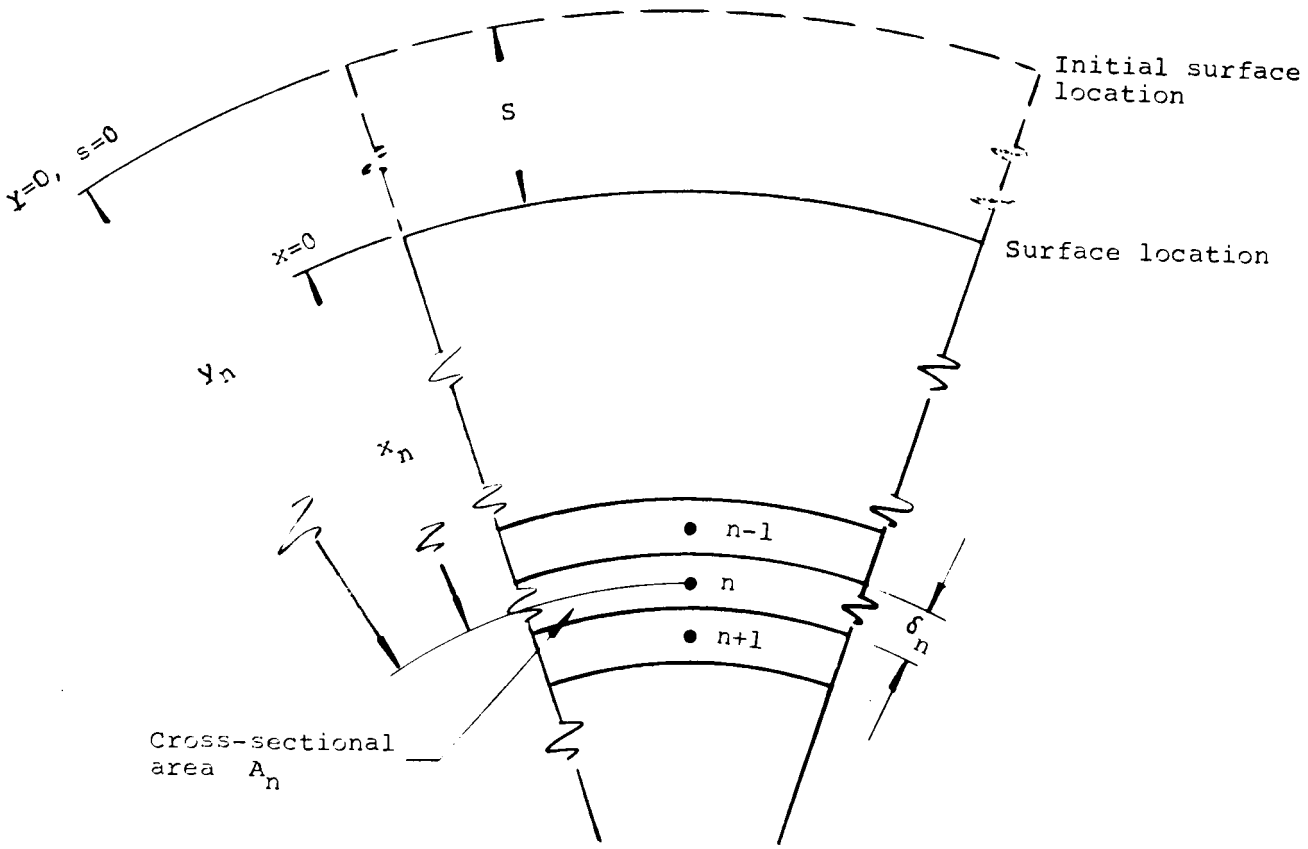

Figure 4. Coordinate System and Finite Difference Representation for Numerical Solution

APPENDIX A

DEVELOPMENT OF RATE EQUATION FOR CHARACTERIZING DECOMPOSITION OF ORGANIC CONSTITUENTS

The decomposition rates of organic constituents utilized in ablative materials have been successfully correlated in terms of kinetic equations of the Arrhenius form (Refs. A-1 and A-2). The purpose of this appendix is to develop a kinetic equation of a form convenient for inclusion in a charring material response calculation procedure in terms of quantities readily derived from TGA data.

TGA data are normally interpreted in terms of an idealized irreversible reaction of the form

$$m \xrightarrow{k_f} m_c + m_g \tag{A-1}$$

where m represents the instantaneous sample weight which is decomposing to form a carbonaceous residue, m_c, and pyrolysis gas, m_g. The TGA data are correlated by an equation of the form

$$\frac{d}{d\theta}\left(\frac{m}{m_o}\right) = -k_f e^{-E/RT}\left(\frac{m}{m_o} - \frac{m_{cf}}{m_o}\right)^n \tag{A-2}$$

where

m = instantaneous sample weight

m_o = initial sample weight

m_{cf} = final weight of carbonaceous residue after decomposition

k_f = pre-exponential constant for the reaction

n = reaction order

E = activation energy

The reaction rate coefficients in the above equation are derived directly from TGA data, however, the equation is not suitable, in its present form, for inclusion in a computational scheme where consideration is given to a number of simultaneous decomposition reactions. This is the case because Eq. (A-2) contains the carbon residue mass (m_{cf}). If decomposition of a mixture of constituents is considered, each characterized by Eq. (A-2), then it would be necessary to keep track of the carbon residue that has resulted from decomposition of each constituent. This requires extra computational effort, which, as will be shown, is not necessary. It is desired to express

the decomposition rate of each reactant in terms of the reactant mass rather than the total mass of reactant and char residue. In Eq. (A-2) the total mass at any instant, m, represents the mass of undecomposed reactant, m_r, plus the mass of char residue, m_c.

$$m = m_r + m_c \tag{A-3}$$

The sketch below depicts the masses m_r and m_c as a function of the total mass, m

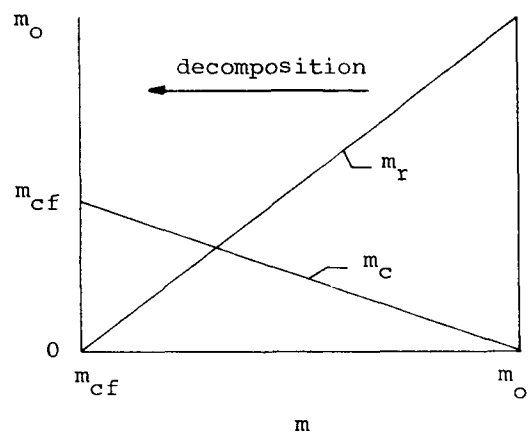

It is noted that initially, before decomposition,

$$m = m_r = m_o$$

and finally, after decomposition is complete

$$m = m_{cf} = m_c$$

The rate of consumption of reactant may be related to the total mass loss rate as follows

$$\frac{dm_r}{d\theta} = \frac{dm_r}{dm}\frac{dm}{d\theta} \tag{A-4}$$

Utilizing the above sketch it is noted that

$$\frac{dm_r}{dm} = \left(\frac{m_o}{m_o - m_{cf}}\right) \tag{A-5}$$

Substituting (A-4) in (A-5) yields

$$\frac{dm_r}{d\theta} = \left(\frac{m_o}{m_o - m_{cf}}\right)\frac{dm}{d\theta} \tag{A-6}$$

Substituting (A-6) in (A-2) results in an expression for the rate of reactant consumption

$$\frac{d}{d\theta}\left(\frac{m_r}{m_o}\right) = - k_f e^{-E/RT}\left(\frac{m_o}{m_o - m_{cf}}\right)\left(\frac{m - m_{cf}}{m_o}\right)^n \tag{A-7}$$

Rearranging and integrating Eq. (A-5) obtains

$$\int_{m_r}^{o} dm_r = \left(\frac{m_o}{m_o - m_{cf}}\right)\int_{m}^{m_{cf}} dm \tag{A-8}$$

from which

$$m - m_{cf} = \left(\frac{m_o - m_{cf}}{m_o}\right)m_r \tag{A-9}$$

Substituting in Eq. (A-7) yields

$$\frac{d}{d\theta}\left(\frac{m_r}{m_o}\right) = - k_f e^{-E/RT}\left(\frac{m_o}{m_o - m_{cf}}\right)^{1-n}\left(\frac{m_r}{m_o}\right)^n \tag{A-10}$$

The above is the desired form of the decomposition rate equation for a system having several reactive constituents because it contains neither the total mass, m, nor the mass of char residue at any instant, m_c. Utilization of Eq. (A-2) directly would require keeping track of the quantity of carbon residue resulting from each of a number of decomposition reactions. Since the decomposition rate clearly depends upon the quantity of reactant present and not upon the quantity of carbon previously formed from the reaction, Eq. (A-10) is simpler to use in a computational scheme.

Rewriting Eq. (A-10) for the i^{th} reactant and defining mass fractions on the basis of the initial mass, m_o, yields

$$\frac{dK_i^o}{d\theta} = -k_{fi} e^{-E_i/RT} \left(1 - K_{c_{if}}^o\right)^{n_i - 1} \left(K_i^o\right)^{n_i} \qquad \text{(A-11)}$$

where

K_i^o = (m_i/m_{io}) mass of i per unit mass of i prior to decomposition

$K_{c_{if}}^o$ = $(m_{c_{if}}/m_{io})$ mass of carbon residue after complete decomposition per unit mass of i prior to decomposition

It is noted that both k_{fi} and $K_{c_{if}}$ are constant for a given reactant, and, as such, it is convenient to combine them into a single effective rate coefficient, k_i.

$$\frac{dK_i^o}{d\theta} = -k_i e^{-E_i/RT} (K_i^o)^{n_i} \qquad \text{(A-12)}$$

where

$$k_i = k_{fi} \left(1 - K_{c_{if}}^o\right)^{n_i - 1}$$

REFERENCES TO APPENDIX A

A-1 Goldstein, H. E.: Kinetics of Nylon and Phenolic Pyrolysis. Lockheed Missiles and Space Company, Sunnyvale, California, LMSC-667876, October 1965.

A-2 Farmer, R. W.: Thermogravimetry of Plastics. ASD-TDR-62-1043, February 1963.